

Article

# Rational and Semi-Rational Solutions to the (2 + 1)-Dimensional Maccari System

Yong Zhang, Huan-He Dong and Yong Fang \* 

College of Mathematics and Systems Science, Shandong University of Science and Technology,  
Qingdao 266590, China

\* Correspondence: fangyong@sdust.edu.cn

**Abstract:** The KP hierarchy reduction method is one of the most reliable and efficient techniques for determining exact solitary wave solutions to nonlinear partial differential equations. In this paper, according to the KP hierarchy reduction technique, rational and some other semi-rational solutions to the (2 + 1)-dimensional Maccari system are investigated. It is shown that two different types of breathers can be derived, and under appropriate parameter constraints, they can be reduced to some well known solutions, involving the homoclinic orbits, dark soliton or anti-dark soliton solution. For the dark and anti-dark solution, its interaction is similar to a resonance soliton. Furthermore, by using a limiting technique, we derive two kinds of rational solutions, one is the lump and the other one is the rogue wave. After constructing these solutions, we further discuss the interactions between the obtained solutions. It is interesting that we obtain a parallel breather and a intersectional breather, which seems very surprising. Finally, we also provide a new three-state interaction, which is composed by the dark-soliton, rogue wave and breather and has never been provided for the Maccari system.

**Keywords:** maccari system; KP hierarchy reduction technique; breather; rational solutions



**Citation:** Zhang, Y.; Dong, H.-H.; Fang, Y. Rational and Semi-Rational Solutions to the (2 + 1)-Dimensional Maccari System. *Axioms* **2022**, *11*, 472. <https://doi.org/10.3390/axioms11090472>

Academic Editor: Ravi P. Agarwal

Received: 17 August 2022

Accepted: 10 September 2022

Published: 15 September 2022

**Publisher's Note:** MDPI stays neutral with regard to jurisdictional claims in published maps and institutional affiliations.



**Copyright:** © 2022 by the authors. Licensee MDPI, Basel, Switzerland. This article is an open access article distributed under the terms and conditions of the Creative Commons Attribution (CC BY) license (<https://creativecommons.org/licenses/by/4.0/>).

## 1. Introduction

Within nonlinear science, soliton theory is very important. Since this concept was introduced, much work on integrable systems has been performed. In recent years, some interesting localized waves were obtained, such as soliton [1–4], traveling wave [5–9], lump solution [10–12], rogue wave [13–20] and breather [21–24]. Due to the balance between the nonlinear term and the dispersion, we know that a solitary wave is a stable wave [2,3]. The travelling wave solution is the group-invariant solution of the space-time translation group, which is suitable for a physical system whose space-time translation is invariant. The lump in the (2 + 1)-dimensional system is similar to the rogue wave in the (1 + 1)-dimensional system [11]. On the other hand, the rogue wave for the (2 + 1)-dimensional system contains the localized type and the line rogue wave, and was observed in the deep ocean firstly and appears from nowhere and disappears without trace [13,14]. The Kuznetsov–Ma breather is periodic in time, and decreases exponentially in space [4,21]. The Akhmediev breather behaves very differently, as it is localized in time and periodic in space [23]. The so called Peregrine breather is actually a rogue wave, and it is localized in both time and space [22]. There are differences between the three kinds of breathers, but they are related in some modes of symmetry reduction. That is, the Peregrine breather can be considered as a limit solution of the Kuznetsov–Ma breather or the Akhmediev breather. Specifically, homoclinic orbits have attracted much attention in deterministic nonlinear dynamics [25,26], and can also be regarded as special breathers. Ablowitz et al. provided some research on the homoclinic structure of the nonlinear Schrödinger (NLS) equation, which is closely related to the  $N$ -soliton solutions of Hirota. It is astounding that the homoclinic orbits of the focusing NLS equation are associated with the dark solitons of the defocusing NLS

equation [26]. Thus, we can say that the breather is very important in the integrable system and the homoclinic orbits solution, as the lump solution and rogue are all related to it.

In this paper, we pay attention to the Maccari system [27]

$$\begin{aligned} L_y &= A_x A^* + A A_x^*, \\ iA_t + LA + A_{xx} &= 0 \end{aligned} \tag{1}$$

where the superscript \* in  $A^*$  indicates the conjugate. Like to the Yajima-Oikawa system [28], this system also describes the interaction between the long wave and the short wave. Additionally, this system is usually used to describe the motion of the solitary wave, localized in a small part of space, in some fields such as hydrodynamics, plasma physics and nonlinear optics. Lai et al. obtained its two-dromion solutions using the technique of the coalescence of wavenumbers [29]. Based on singularity structure analysis, Uthayakumar et al. studied the integrability property of this system [30]. It is well known that there is much research on the Maccari system; however, to our knowledge, there are less systematic studies on the breather as well as the the corresponding interactions to this system. Therefore, based on the KP reduction method, we provide a systematic study on the breathers of the Maccari system and then further analyze the interactions between some localized waves.

As to these two classical breathers, the Akhmediev breather and Kuznetsov–Ma breather, their solutions can interconvert with each other by using a wave number transformation ( $k_i \rightarrow ik_i$ ). The Maccari system also has two corresponding breather solutions with the wave number transformation ( $\mu_{2k-1} \rightarrow i\mu_{2k-1}, \mu_{2k} \rightarrow -i\mu_{2k}, \omega_{2k-1} \rightarrow i\omega_{2k-1}, \omega_{2k} \rightarrow -i\omega_{2k}$ ). However, the dynamics of these two breathers are different, as one is localized in the  $x$ -direction and periodic in the  $y$ -direction and the other one has an opposite characteristic. Furthermore, under some special parameter constraints, we can derive some other localized waves, involving the homoclinic orbits solution, dark soliton solution, anti-dark soliton solution, lump solution and rogue wave. After that, we also provide some interactions for these obtained solutions.

The structure of this paper is as follows. Section 2 provides the bilinear form and Gram determinant solution of the Maccari system. Section 3 discusses one type of breather solution, which is localized in one spatial variable and periodic in the other one. Moreover, we also obtain two rational solutions, the lump solution and rogue wave. Then, some combination solutions between them are provided. Section 4 discusses the other type of breather solution, which has an opposite dynamic to the one in Section 3. Under this condition, the dark soliton, anti-dark soliton, rogue wave as well as some interactions are provided. Finally, we present the conclusions in last section.

## 2. Gram Determinant Solution of Maccari System

We first obtain the bilinear form of Equation (1) as

$$\begin{aligned} D_x D_y f \cdot f + q^2 (f^2 - g g^*) &= 0, \\ (D_x^2 + iD_t) g \cdot f &= 0, \end{aligned} \tag{2}$$

by introducing a new variables transformation

$$\begin{aligned} A &= \frac{q \exp(-ibt)g}{f}, \\ L &= 2(\ln f)_{xx} - b, \end{aligned} \tag{3}$$

where  $f$  is a real variable,  $g$  is a complex one, and the  $D$  is the Hirota bilinear operator is defined as

$$D_t^m D_x^n (a, b) = \frac{\partial^m}{\partial s^m} \frac{\partial^n}{\partial r^n} a(t + s, x + r) b(t - s, x - r) \Big|_{s=0, r=0}.$$

In Ref. [31], the authors provide a detailed calculation for the regularity of  $f$  and in Ref. [32], the authors prove its regularity systematically.

Our primary goal is to construct the localized wave solutions for the Maccari system. Additionally, we use the classical KP reduction technique. To realize this, we try to use the bilinear equations from the KP hierarchy as follows

$$\begin{aligned} (D_{x_1}^2 - D_{x_2})v(k+1)v(k) &= 0, \\ (D_{x_1}D_{x_{-1}} - 2)v(k)v(k) &= -2v(k+1)v(k-1), \end{aligned} \tag{4}$$

which has been proved to have the Gram determinant solutions

$$v(k) = |\hat{m}_{ij}(k)|_{1 \leq i, j \leq N} \tag{5}$$

and the entries of the determinant are the following formulas,

$$\begin{aligned} \hat{m}_{ij}(k) &= c_{ij} + \frac{1}{\mu_i + \omega_j} \hat{\phi}_i(k) \hat{\psi}_j(k), \\ \hat{\phi}_i(k) &= (\mu_i - a)^k (\mu_i + \omega_i) \exp(r_i), \\ \hat{\psi}_j(k) &= \left( \frac{-1}{\omega_j + a} \right)^k \exp(s_j) \end{aligned}$$

with

$$\begin{aligned} r_i &= \frac{1}{\mu_i - a} x_{-1} + \mu_i x_1 + \mu_i^2 x_2 + r_{i0}, \\ s_j &= \frac{1}{\omega_j + a} x_{-1} + \omega_j x_1 - \omega_j^2 x_2 + s_{j0} \end{aligned}$$

where  $c_{ij}, \mu_i, \omega_j, r_{i0}, s_{j0}$  are complex constant.

Taking the variable transformation

$$x_1 = ix, x_2 = it, x_{-1} = \frac{Q^2 y}{2},$$

i.e.,

$$\partial_{x_1} = -i\partial_x, \partial_{x_2} = -i\partial_t, \partial_{x_{-1}} = \frac{-2i}{Q^2} \partial_y,$$

and defining the function in Equation (4) as

$$f = v(0), g = v(1), \tilde{g} = v(-1), \tilde{g} = g^*, \tag{6}$$

we can derive the bilinear equation in Equation (2) from the KP hierarchy in Equation (4).

Therefore, by replacing the function  $g^*$  with  $\tilde{g}$ , the Gram determinants solution of Equation (3) can be obtained as

$$\begin{aligned} f &= \left| \delta_{ij} + \frac{\mu_i + \omega_i}{\mu_i + \omega_j} \exp(\zeta_i + \eta_j) \right| \\ g &= \left| \delta_{ij} + \left( -\frac{\mu_i - a}{\omega_j + a} \right) \frac{\mu_i + \omega_i}{\mu_i + \omega_j} \exp(\zeta_i + \eta_j) \right| \\ \tilde{g} &= \left| \delta_{ij} + \left( -\frac{\omega_j + a}{\mu_i - a} \right) \frac{\mu_i + \omega_i}{\mu_i + \omega_j} \exp(\zeta_i + \eta_j) \right| \end{aligned} \tag{7}$$

where

$$\zeta_i = \frac{\rho^2 i}{2(\mu_i - a)} y + \mu_i i x - \mu_i^2 i t + \zeta_{i,0},$$

$$\eta_j = \frac{\rho^2 i}{2(\omega_j - a)} y + \omega_j i x + \omega_j^2 i t + \eta_{j,0}.$$

To satisfy our bilinear equation, we should implement the constraint condition  $\tilde{g} = g^*$ , which was verified in Ref. [24]. It should be noted that the integer  $N$  in Equation (5) should be even, namely,  $N = 2M$ . Furthermore, we should also let it satisfy the complex conjugate condition, for which the detailed calculations are shown in the following sections.

### 3. Breather I

In Appendix A, the Breather I to the Maccari system is provided. It can be seen that the exact solutions are very complex, and for simplicity, we only list the first two types, that is, one-breather and two-breather.

(i) Take  $M = 1$  in Equation (A2), then the breather is

$$A = \frac{\rho \exp(-ibt)g}{f},$$

$$L = 2(\ln f)_{xx} - b,$$

$$f = 1 + \exp(\Psi_1) + \exp(\Psi_1^*) + A_{12} \exp(\Psi_1 + \Psi_1^*), \tag{8}$$

$$g = 1 + \frac{2\Phi_1 + 2a - \phi_1}{2\Phi_1 + 2a + \phi_1} \exp(\Psi_1) + \frac{2\Phi_1^* + 2a + \phi_1}{2\Phi_1^* + 2a - \phi_1} \exp(\Psi_1^*) + A_{12} \frac{2\Phi_1 + 2a - \phi_1}{2\Phi_1 + 2a + \phi_1} \frac{2\Phi_1^* + 2a + \phi_1}{2\Phi_1^* + 2a - \phi_1} \exp(\Psi_1 + \Psi_1^*)$$

where  $A_{12} = 1 - \frac{\phi_1^2}{(\Phi_1 - \Phi_1^*)^2}$ ,  $\Psi_1 = i\phi_1 x + 2i\phi_1 \Phi_1 t - \frac{2i\phi_1 \rho^2}{4\Phi_1^2 - \phi_1^2} y + \Psi_{1,0}$ .

Let  $\Phi_1 = \Phi_{1R} + i\Phi_{1I}$ , then the corresponding  $\Psi_1$  can be written as  $\Psi_1 = \Psi_{1R} + i\Psi_{1I}$ , where

$$\Psi_{1R} = -2\phi_1 \Phi_{1I} \left[ t + \frac{8\rho^2 \Phi_{1R}}{[4(\Phi_{1R}^2 - \Phi_{1I}^2) - \phi_1^2]^2 + 64\Phi_{1R}\Phi_{1I}} y \right] + \Psi_{1,0},$$

$$\Psi_{1I} = \phi_1 \left[ x + 2\Phi_{1R} t + \frac{2\rho^2 (\phi_1^2 + 4\Phi_{1I}^2 - 4\Phi_{1R}^2)}{[4(\Phi_{1R}^2 - \Phi_{1I}^2) - \phi_1^2]^2 + 64\Phi_{1R}\Phi_{1I}} y \right].$$

It is easy to find that when  $\Psi_{1R} \rightarrow -\infty, L \rightarrow -b, A \rightarrow \rho \exp(-ibt)$  and when  $\Psi_{1R} \rightarrow +\infty, L \rightarrow -b, A \rightarrow \rho \exp(-ibt) \frac{(2\Phi_{1R} + 2a - \phi_1 + 2i\Phi_{1I})(2\Phi_{1R} + 2a + \phi_1 - 2i\Phi_{1I})}{(2\Phi_{1R} + 2a + \phi_1 + 2i\Phi_{1I})(2\Phi_{1R} + 2a - \phi_1 - 2i\Phi_{1I})}$ ; thus, we know that the line  $\Psi_{1R}$  will determine the localized property and line  $\Psi_{1I}$  will affect the periodic property. Moreover, these two properties are controlled by the common parameters  $\Phi_{1R}, \Phi_{1I}, \phi_1, \rho$ . By setting the time  $t = 0$ , we obtain the breather of Equation (3) in Figure 1.

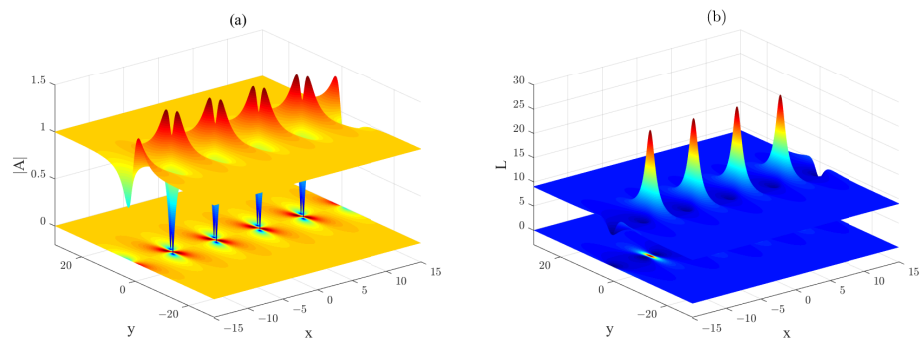


**Figure 1.** One kind of breather to the Maccari system is found with  $a = 0, b = -10, \rho = 1, \Phi_{1R} = 1, \Phi_{1I} = 1, \phi_1 = 1, \Psi_{1,0} = 0$ : (a) short wave component  $A$ ; (b) long wave component  $L$ .

Then, by choosing another different parameter, we provide the evolution progress of homoclinic orbits in Figure 2. We only provide a simple example for one-breather, and this character can also be seen in some multi-breathers.

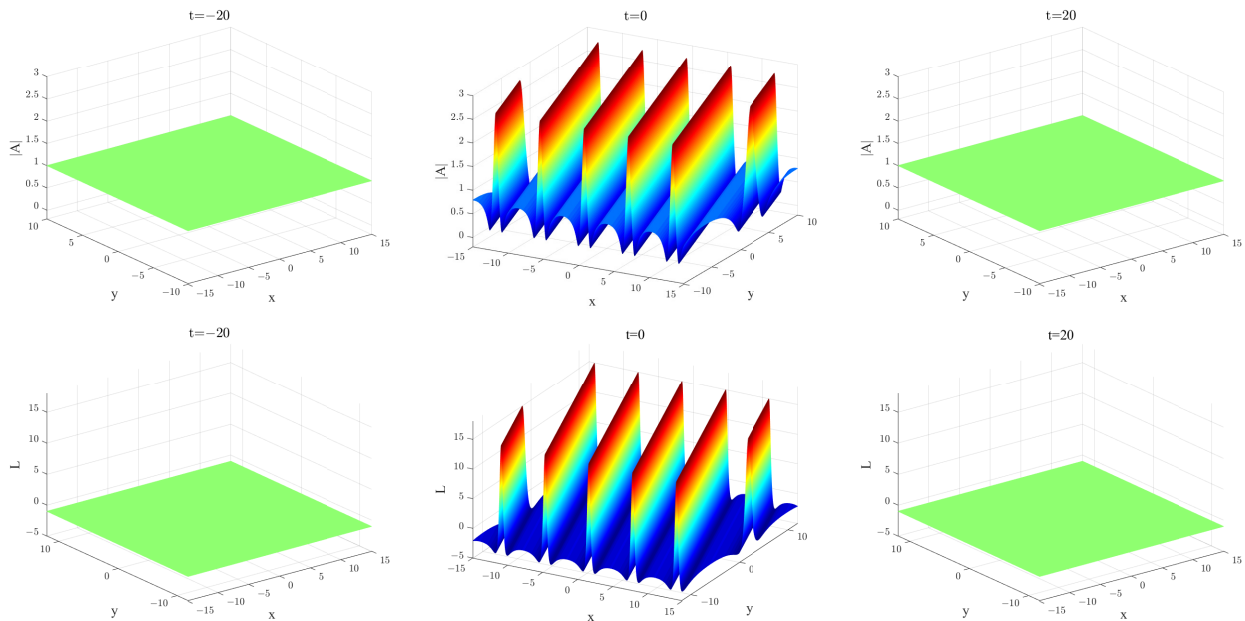


**Figure 2.** The evolution homoclinic orbits to Maccari system by choosing  $a = 0, b = 1, \rho = 1, \Phi_{1R} = 0, \Phi_{1I} = 1, \phi_1 = 1, \Psi_{1,0} = 0$ .

Now, we provide a brief description of this homoclinic orbit. From the expression of  $\Psi_{1R}$  and its figures, we know that it involves two variables,  $y$  and  $t$ . Thus, it is easy to know that if the spatial variable  $y$  vanishes, the localized behavior can only be determined by the time variable. Then, this solution will be different from the general breather. When  $t$  is large, it will approach a constant background, and then it will appear as periodic waves, but when  $t$  is large, it will revert to the same constant background. Thus, we call them homoclinic orbits.

(ii) When  $M = 2$ , the two-breather solution to Equation (3) is

$$A = \frac{\varrho \exp(-ibt)g}{f},$$

$$L = 2(\ln f)_{xx} - b,$$

$$f = B \begin{vmatrix} \frac{1}{\phi_1 \exp(\Psi_1)} + \frac{1}{\phi_1} & \frac{1}{\Phi_1^* - \Phi_1} & \frac{1}{\Phi_2 - \Phi_1 + \frac{\phi_1 + \phi_2}{2}} & \frac{1}{\Phi_2^* - \Phi_1 + \frac{\phi_1 - \phi_2}{2}} \\ \frac{1}{\Phi_1^* - \Phi_1} & \frac{1}{\phi_1 \exp(\Psi_1^*)} + \frac{1}{\phi_1} & \frac{1}{\Phi_1^* - \Phi_2 + \frac{\phi_1 - \phi_2}{2}} & \frac{1}{\Phi_1^* - \Phi_2^* + \frac{\phi_1 + \phi_2}{2}} \\ \frac{1}{\Phi_1 - \Phi_2 + \frac{\phi_1 + \phi_2}{2}} & \frac{1}{\Phi_1^* - \Phi_2 - \frac{\phi_1 - \phi_2}{2}} & \frac{1}{\phi_2 \exp(\Psi_2)} + \frac{1}{\phi_2} & \frac{1}{\Phi_2^* - \Phi_2} \\ \frac{1}{\Phi_2^* - \Phi_1 - \frac{\phi_1 - \phi_2}{2}} & \frac{1}{\Phi_2^* - \Phi_1^* + \frac{\phi_1 + \phi_2}{2}} & \frac{1}{\Phi_2^* - \Phi_2} & \frac{1}{\phi_2 \exp(\Psi_2^*)} + \frac{1}{\phi_2} \end{vmatrix} \tag{9}$$

$$g = B \begin{vmatrix} \frac{1}{\phi_1 \exp(\Psi_1)} + \frac{1}{\phi_1} \frac{\Phi_1 + a - \frac{\phi_1}{2}}{\Phi_1 + a + \frac{\phi_1}{2}} & \frac{1}{\Phi_1^* - \Phi_1} \frac{\Phi_1 + a - \frac{\phi_1}{2}}{\Phi_1^* + a - \frac{\phi_1}{2}} & \frac{1}{\Phi_2 - \Phi_1 + \frac{\phi_1 + \phi_2}{2}} \frac{\Phi_1 + a - \frac{\phi_1}{2}}{\Phi_2 + a + \frac{\phi_2}{2}} & \frac{1}{\Phi_2^* - \Phi_1 + \frac{\phi_1 - \phi_2}{2}} \frac{\Phi_1 + a - \frac{\phi_1}{2}}{\Phi_2^* + a - \frac{\phi_2}{2}} \\ \frac{1}{\Phi_1^* - \Phi_1} \frac{\Phi_1 + a + \frac{\phi_1}{2}}{\Phi_1 + a + \frac{\phi_1}{2}} & \frac{1}{\phi_1 \exp(\Psi_1^*)} + \frac{1}{\phi_1} \frac{\Phi_1^* + a + \frac{\phi_1}{2}}{\Phi_1^* + a - \frac{\phi_1}{2}} & \frac{1}{\Phi_1^* - \Phi_2 + \frac{\phi_1 - \phi_2}{2}} \frac{\Phi_1^* + a + \frac{\phi_1}{2}}{\Phi_2 + a + \frac{\phi_2}{2}} & \frac{1}{\Phi_1^* - \Phi_2^* + \frac{\phi_1 + \phi_2}{2}} \frac{\Phi_1^* + a + \frac{\phi_1}{2}}{\Phi_2^* + a - \frac{\phi_2}{2}} \\ \frac{1}{\Phi_1 - \Phi_2 + \frac{\phi_1 + \phi_2}{2}} \frac{\Phi_2 + a - \frac{\phi_2}{2}}{\Phi_1 + a + \frac{\phi_1}{2}} & \frac{1}{\Phi_1^* - \Phi_2 - \frac{\phi_1 - \phi_2}{2}} \frac{\Phi_2 + a - \frac{\phi_2}{2}}{\Phi_1^* + a - \frac{\phi_1}{2}} & \frac{1}{\phi_2 \exp(\Psi_2)} + \frac{1}{\phi_2} \frac{\Phi_2 + a - \frac{\phi_2}{2}}{\Phi_2 + a + \frac{\phi_2}{2}} & \frac{1}{\Phi_2^* - \Phi_2} \frac{\Phi_2 + a - \frac{\phi_2}{2}}{\Phi_2^* + a - \frac{\phi_2}{2}} \\ \frac{1}{\Phi_2^* - \Phi_1 - \frac{\phi_1 - \phi_2}{2}} \frac{\Phi_2^* + a + \frac{\phi_2}{2}}{\Phi_1 + a + \frac{\phi_1}{2}} & \frac{1}{\Phi_2^* - \Phi_1^* + \frac{\phi_1 + \phi_2}{2}} \frac{\Phi_2^* + a + \frac{\phi_2}{2}}{\Phi_1^* + a - \frac{\phi_1}{2}} & \frac{1}{\Phi_2^* - \Phi_2} \frac{\Phi_2^* + a + \frac{\phi_2}{2}}{\Phi_2 + a + \frac{\phi_2}{2}} & \frac{1}{\phi_2 \exp(\Psi_2^*)} + \frac{1}{\phi_2} \frac{\Phi_2^* + a + \frac{\phi_2}{2}}{\Phi_2^* + a - \frac{\phi_2}{2}} \end{vmatrix}$$

where

$$\Psi_1 = i\phi_1 x + 2i\phi_1 \Phi_1 t - \frac{2i\phi_1 \varrho^2}{4\Phi_1^2 - \phi_1^2} y + \Psi_{1,0},$$

$$\Psi_2 = i\phi_2 x + 2i\phi_2 \Phi_2 t - \frac{2i\phi_2 \varrho^2}{4\Phi_2^2 - \phi_2^2} y + \Psi_{2,0},$$

$$B = \exp(\Psi_1 + \Psi_1^* + \Psi_2 + \Psi_2^*) \phi_1^2 \phi_2^2.$$

Since there are two different types of breathers for one-breather, it is easy to know that three types of interactions will exist between the two-breather. One is the interaction between two different kinds of one-breather, and the other two are the same types. To demonstrate this clearly, we provide the dynamics in Figures 3–5.

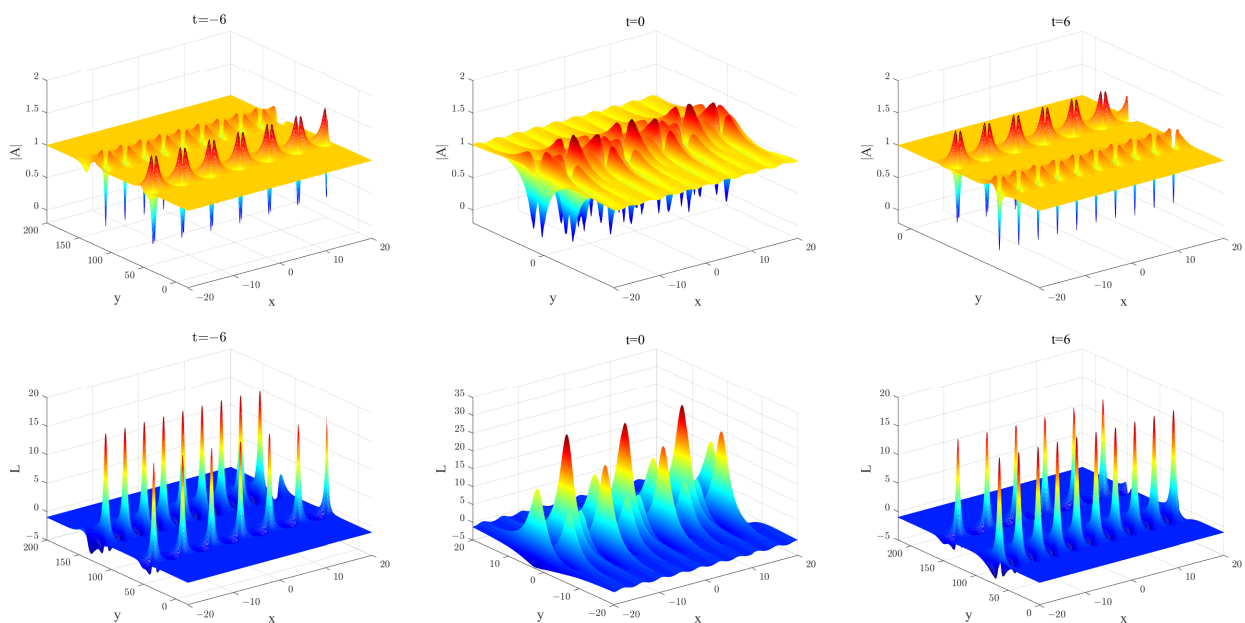


**Figure 3.** Two general breathers to Maccari system by choosing  $a = 0, b = 1, \varrho = 1, \Phi_{1R} = 1, \Phi_{1I} = 1, \phi_1 = 1, \Phi_{2R} = 2, \Phi_{2I} = 1, \phi_2 = -\frac{3}{2}, \Psi_{1,0} = 0, \Psi_{2,0} = 0$ .

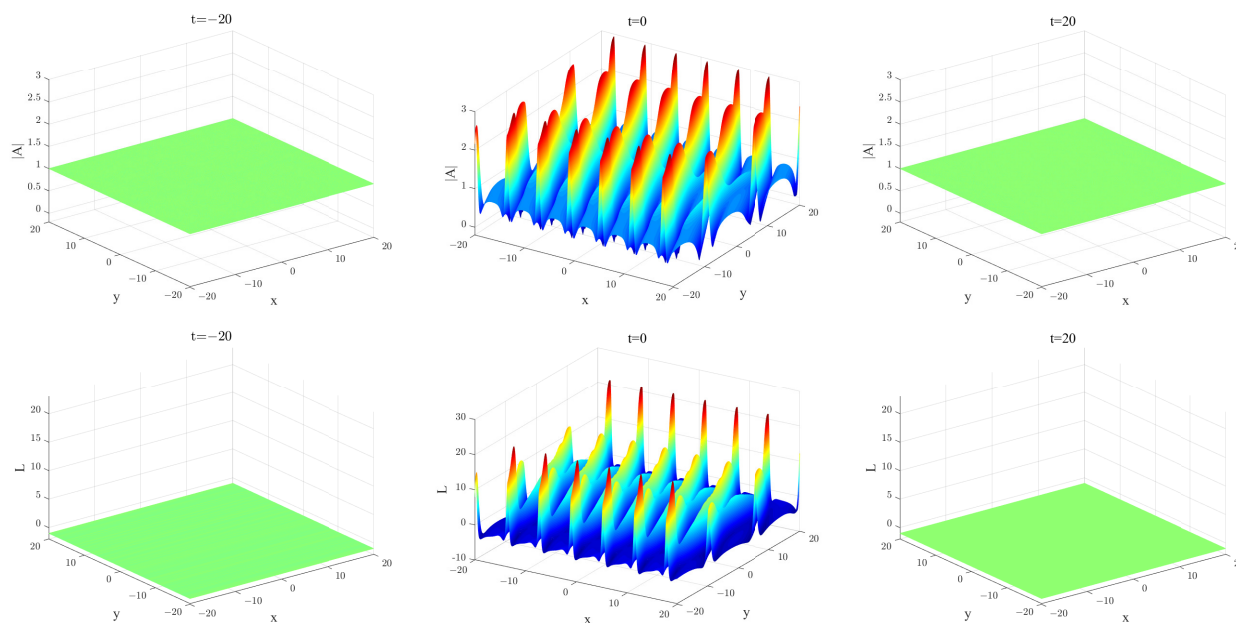


**Figure 4.** The evolutive dynamics of two homoclinic orbits to Maccari system by choosing  $a = 0, b = 1, \varrho = 1, \Phi_{1R} = 1, \Phi_{1I} = 2, \phi_1 = 1, \Phi_{2R} = 0, \Phi_{2I} = 1, \phi_2 = -1, \Psi_{1,0} = 0, \Psi_{2,0} = 0$ .

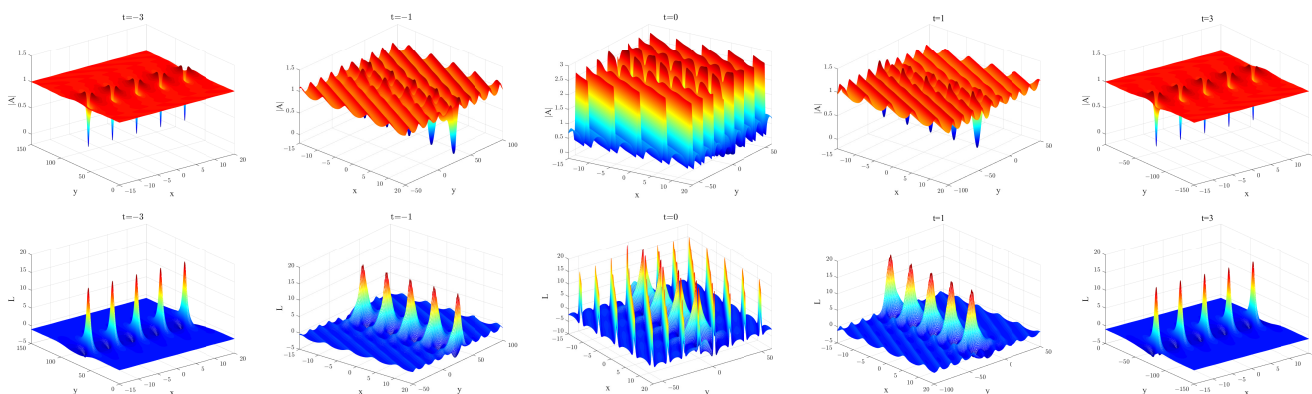


**Figure 5.** The evolution progress to the interaction of general breather and homoclinic orbits to Maccari system by choosing  $a = 0, b = 1, \varrho = 1, \Phi_{1R} = 2, \Phi_{1I} = 1, \phi_1 = 1, \Phi_{2R} = 0, \Phi_{2I} = 1, \phi_2 = -1, \Psi_{1,0} = 0, \Psi_{2,0} = 0$ .

In Figure 3 we can see that since the periodicity only occurs in the  $x$ -direction, the two general breather solutions must be parallel, as time goes on, they go through a similar elastic collision and then they will separate from each other. Figure 4 shows the dynamics of two homoclinic orbits. When  $t$  is large, they approach a constant background, and when  $t$  gets smaller, it appears a beautiful interaction, and then they will go back to the constant background. The interaction between the breather and the homoclinic orbit is more interesting, they have their own inherent characteristics and they also affect the other ones. Especially, this interaction is the strongest at  $t = 0$ . In addition, the amplitudes of the long wave and the short wave are also different. As to the long wave component  $L$ , the maximum amplitude of the homoclinic orbit can equal to the general breather, but the amplitude of homoclinic orbit is shorter than the general breather all the time for the short wave.

We have discussed the breather solutions of Equation (1) above, and then we derive its rational solution. By using a limit skill, we gain the rational solution to the Maccari system in Appendix B.

(i) Set  $M = 1$  in Equation (A5), then the rational solution can be given as

$$\begin{aligned}
 f &= |\omega_1|^2 - \frac{1}{(\Phi_1 - \Phi_1^*)^2}, \\
 g &= \left(\omega_1 - \frac{1}{\Phi_1 + a}\right) \left(\omega_1^* + \frac{1}{\Phi_1^* + a}\right) - \frac{1}{(\Phi_1 - \Phi_1^*)^2}
 \end{aligned}
 \tag{10}$$

with

$$\omega_1 = ix + 2i\Phi_{1R}t - \frac{2iq^2}{4\Phi_{1I}^2}y.$$

By letting  $\Phi_1 = \Phi_{1R} + i\Phi_{1I}$ , the rational solution can be equal to the following formula

$$\begin{aligned}
 f &= |\omega_1|^2 + \frac{1}{4\Phi_{1I}^2}, \\
 g &= (\omega_1 + m_1 + im_2)(\omega_1^* - m_1 + im_2) + \frac{1}{4\Phi_{1I}^2},
 \end{aligned}
 \tag{11}$$

where  $\omega_1 = ix + (2i\Phi_{1R} - 2\Phi_{1I})t - (in_1 + n_2)y$ , with

$$\begin{aligned}
 m_1 &= -\frac{a + \Phi_{1R}}{(a + \Phi_{1R})^2 + \Phi_{1I}^2}, \\
 m_2 &= \frac{\Phi_{1I}}{(a + \Phi_{1R})^2 + \Phi_{1I}^2}, \\
 n_1 &= \frac{q^2(\Phi_{1R}^2 - \Phi_{1I}^2)}{2(\Phi_{1R}^2 - \Phi_{1I}^2)^2 + 8\Phi_{1R}\Phi_{1I}}, \\
 n_2 &= \frac{2q^2\Phi_{1R}\Phi_{1I}}{2(\Phi_{1R}^2 - \Phi_{1I}^2)^2 + 8\Phi_{1R}\Phi_{1I}}.
 \end{aligned}$$

Substituting it to Equation (3), we can get the rational solution of  $A$  and  $L$  as

$$\begin{aligned}
 A &= q \exp(-ibt) \left[ 1 - \frac{2im_1(x + 2\Phi_{1R}t - n_1y) + 2im_2(2\Phi_{1I}t + n_2y) + m_1^2 + m_2^2}{(x + 2\Phi_{1R}t - n_1y)^2 + (2\Phi_{1I}t + n_2y)^2 + \frac{1}{4\Phi_{1I}^2}} \right], \\
 L &= -4 \frac{(x + 2\Phi_{1R}t - n_1y)^2 - (2\Phi_{1I}t + n_2y)^2 - \frac{1}{4\Phi_{1I}^2}}{\left[ (x + 2\Phi_{1R}t - n_1y)^2 + (2\Phi_{1I}t + n_2y)^2 + \frac{1}{4\Phi_{1I}^2} \right]^2} - b.
 \end{aligned}
 \tag{12}$$

Next, we give a detailed analysis for the lump solution and the rogue wave, whose figures are shown in Figures 6 and 7.

(1) Lump solution. By a simple calculation, we easily see that when

$$\begin{aligned}
 x + 2\Phi_{1R}t - n_1y &= 0, \\
 2\Phi_{1I}t + n_2y &= 0,
 \end{aligned}$$

we have  $[A, L] \rightarrow [q \exp(-ibt)(1 - 4\Phi_{1I}^2(m_1^2 + m_2^2)), 16\Phi_{1I}^2 - b]$ .

In Figure 6, if we choose a fixed time  $t$ , we can see that  $(A, L) \rightarrow (q \exp(-ibt), -b)$  when  $(x, y) \rightarrow \infty$ . So the lump solution will go back to the constant background.

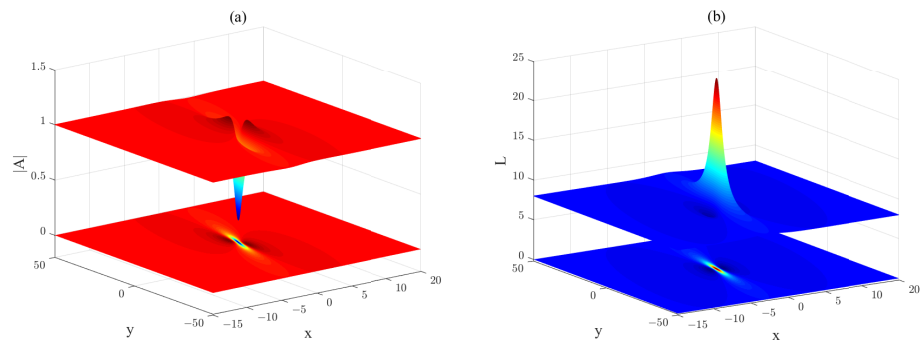


**Figure 6.** The Lump solution to Maccari system at  $t = 0$ , the parameters are chosen as  $a = 0$ ,  $b = -8, \rho = 1, \Phi_{1R} = 2, \Phi_{1I} = -1$ : (a) short wave component  $A$ ; (b) long wave component  $L$ .

(2) Rogue wave. By setting  $n_2 = 0$ , then the dynamics of  $A$  and  $L$  will be different, which are called the line rogue waves.

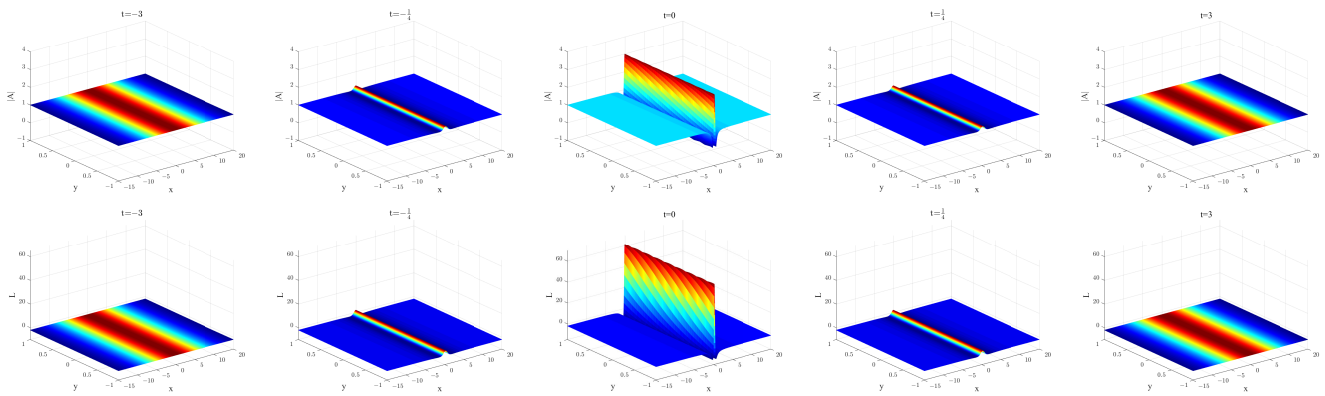


**Figure 7.** The evolution progress of the line rogue wave, the parameters are  $a = 0, b = 2, \rho = 1, \Phi_{1R} = 0, \Phi_{1I} = 2$ .

It is clear that the amplitudes of line rogue wave vary sharply. With a direct calculation, when  $t = 0$  and  $x, y$  satisfies  $x - n_1y = 0$ , the maximum amplitude of  $|A|$  can reach  $\rho(1 - 4\Phi_{1I}^2(m_1^2 + m_2^2))$  and  $L$  is  $(16\Phi_{1I}^2 - b)$ . Precisely, we can also calculate the orientation of this line rogue wave, which is equal to  $\alpha = \tan^{-1}(n_1)$ . And its width is direct proportional to  $\frac{1}{\sqrt{1+n_1^2}}$ . Obviously, these characters can also be observed for the multi-rational solution.

(ii) Set  $M = 2$ , then the two rational solution can be rewritten as

$$\begin{aligned}
 A &= \frac{\rho \exp(-ibt)g}{f}, \\
 u &= 2(\ln f)_{xx} - b, \\
 f &= \begin{vmatrix} \omega_1 & \frac{-1}{\Phi_1 - \Phi_1^*} & \frac{1}{-(\Phi_1 - \Phi_2)} & \frac{1}{-(\Phi_1 - \Phi_2^*)} \\ \frac{-1}{\Phi_1 - \Phi_1^*} & \omega_1^* & \frac{1}{\Phi_1^* - \Phi_2} & \frac{1}{\Phi_1^* - \Phi_2^*} \\ \frac{1}{-(\Phi_2 - \Phi_1)} & \frac{1}{-(\Phi_2 - \Phi_1^*)} & \omega_2 & \frac{-1}{\Phi_2 - \Phi_2^*} \\ \frac{1}{\Phi_2^* - \Phi_1} & \frac{1}{\Phi_2^* - \Phi_1^*} & \frac{-1}{\Phi_2 - \Phi_2^*} & \omega_2^* \end{vmatrix} \\
 g &= \begin{vmatrix} \omega_1 - \frac{1}{\Phi_1 + a} & \frac{-1}{\Phi_1 - \Phi_1^*} \frac{\Phi_1 + a}{\Phi_1^* + a} & \frac{1}{-(\Phi_1 - \Phi_2)} \frac{\Phi_1 + a}{\Phi_2 + a} & \frac{1}{-(\Phi_1 - \Phi_2^*)} \frac{\Phi_1 + a}{\Phi_2^* + a} \\ \frac{-1}{\Phi_1 - \Phi_1^*} \frac{\Phi_1^* + a}{\Phi_1 + a} & \omega_1^* + \frac{1}{\Phi_1^* + a} & \frac{1}{\Phi_1^* - \Phi_2} \frac{\Phi_1^* + a}{\Phi_2 + a} & \frac{1}{\Phi_1^* - \Phi_2^*} \frac{\Phi_1^* + a}{\Phi_2^* + a} \\ \frac{1}{-(\Phi_2 - \Phi_1)} \frac{\Phi_2 + a}{\Phi_1 + a} & \frac{1}{-(\Phi_2 - \Phi_1^*)} \frac{\Phi_2 + a}{\Phi_1^* + a} & \omega_2 - \frac{1}{\Phi_2 + a} & \frac{-1}{\Phi_2 - \Phi_2^*} \frac{\Phi_2 + a}{\Phi_2^* + a} \\ \frac{1}{\Phi_2^* - \Phi_1} \frac{\Phi_2^* + a}{\Phi_1 + a} & \frac{1}{\Phi_2^* - \Phi_1^*} \frac{\Phi_2^* + a}{\Phi_1^* + a} & \frac{-1}{\Phi_2 - \Phi_2^*} \frac{\Phi_2^* + a}{\Phi_2 + a} & \omega_2^* + \frac{1}{\Phi_2^* + a} \end{vmatrix}
 \end{aligned} \tag{13}$$

where

$$\omega_k = ix + 2i\Phi_k t - \frac{2i\varrho^2}{4\Phi_k^2} y \quad (k = 1, 2)$$

Transparently, for the two rational solutions, we can also get three different kinds of interactions, two lump solutions, two rogue waves and the mixed of one lump solution and one rogue wave. By choosing some proper parameters, we give some dynamics behaviors are in Figures 8–10.

In Figure 8, we can see that there are two lump solutions fusion together, which is similar to the collision behavior between two general breather. Figure 9 present the interactions of two rogue waves. Both of them keep their own characters, they arise from a constant background, as the time moves, there are two different line rogue waves, when  $t = 0$ , the interaction is the strongest. When  $t$  is large, they will go back to the constant background again. It is interesting that at the beginning time when these two rogue waves appear, they are intersected, but when  $t = 0$ , there appears an amazing phenomenon, one rogue wave is split up by the other one, which seems very unbelievable. In Figure 10, we give the interaction of one lump soliton and one rogue wave. When  $t$  is large, we only see the lump solution, when  $t$  becomes smaller, the line rogue wave appears. Although the appearing time of rogue wave is transient, the maximal amplitude of rogue wave is much higher than the lump soliton. When  $t$  is large, the line rogue wave disappears again.

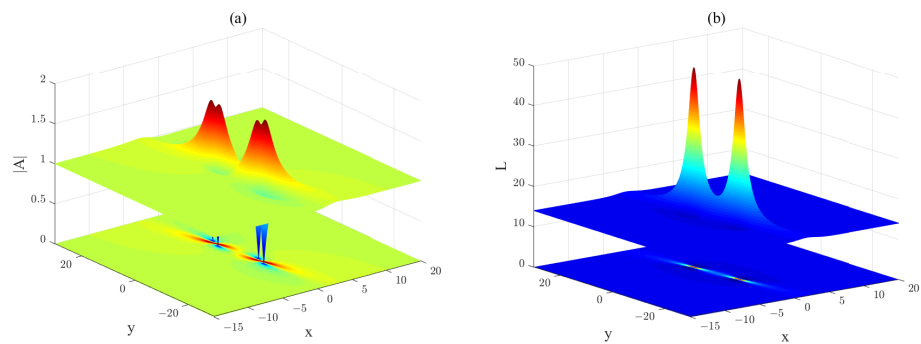


**Figure 8.** Two lump solutions to Maccari system, the parameters are  $t = 0$  and  $a = 0, b = -15, \varrho = 1, \Phi_{1R} = 1, \Phi_{1I} = -\frac{7}{4}, \Phi_{2R} = 1, \Phi_{2I} = 1$ : (a) short wave component  $A$ ; (b) long wave component  $L$ .

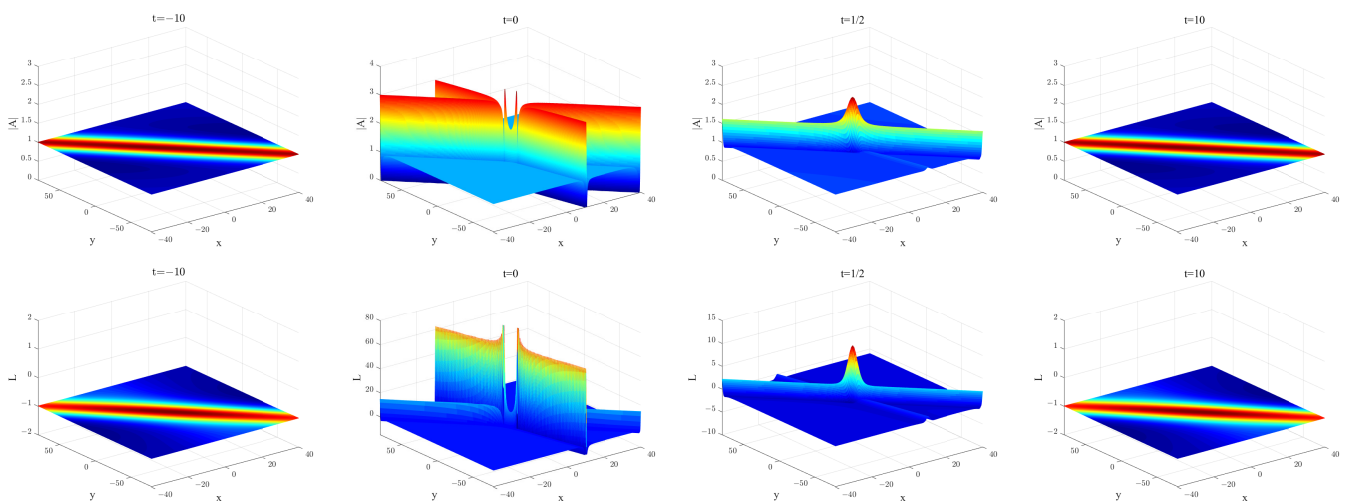


**Figure 9.** The evolution progress of two line rogue waves, the parameters are  $a = 0, b = 1, \varrho = 1, \Phi_{1R} = 0, \Phi_{1I} = 1, \Phi_{2R} = 0, \Phi_{2I} = 2$ .

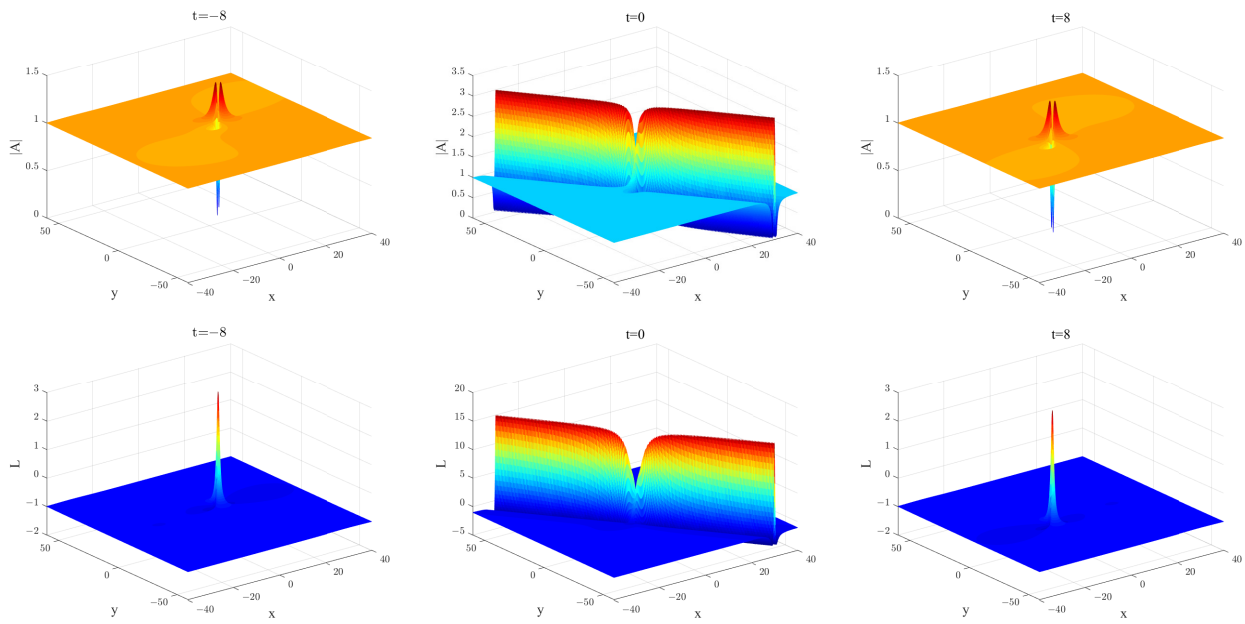


**Figure 10.** The evolution progress of the interaction of lump soliton and line rogue wave, the parameters are chosen as  $a = 0, b = 1, \varrho = 1, \Phi_{1R} = \frac{1}{2}, \Phi_{1I} = \frac{1}{2}, \Phi_{2R} = 0, \Phi_{2I} = 1$ .

Visibly, we construct the breather and rational solution in Appendices A and B. Then we can easily get the combination between these two kinds of solutions, which is given in Appendix C. Now we can give some examples from the exact solution. Setting  $\tilde{N} = 1, \hat{N} = 1$  in Equation (A7), the one-rational-one-exp solution is equal to

$$\begin{aligned}
 A &= \frac{\varrho \exp(-ibt)g}{f}, \\
 u &= 2(\ln(\exp(\Psi_2 + \Psi_2^*)\phi_2^2) \cdot f)_{xx} - b, \\
 f &= \begin{vmatrix} \omega_1 & \frac{-1}{\Phi_1 - \Phi_1^*} & \frac{1}{-(\Phi_1 - \Phi_2) + \frac{\phi_2}{2}} & \frac{1}{-(\Phi_1 - \Phi_2^*) - \frac{\phi_2}{2}} \\ \frac{-1}{\Phi_1 - \Phi_1^*} & \omega_1^* & \frac{1}{(\Phi_1^* - \Phi_2) - \frac{\phi_2}{2}} & \frac{1}{(\Phi_1^* - \Phi_2^*) + \frac{\phi_2}{2}} \\ \frac{1}{-(\Phi_2 - \Phi_1) + \frac{\phi_2}{2}} & \frac{1}{-(\Phi_2 - \Phi_1^*) + \frac{\phi_2}{2}} & \frac{1}{\phi_2 \exp(\Psi_2)} + \frac{1}{\phi_2} & \frac{-1}{\Phi_2 - \Phi_2^*} \\ \frac{1}{(\Phi_2^* - \Phi_1) + \frac{\phi_2}{2}} & \frac{1}{(\Phi_2^* - \Phi_1^*) + \frac{\phi_2}{2}} & \frac{-1}{\Phi_2 - \Phi_2^*} & \frac{1}{\phi_2 \exp(\Psi_2^*)} + \frac{1}{\phi_2} \end{vmatrix} \\
 g &= \begin{vmatrix} \omega_1 - \frac{1}{\Phi_1 + a} & \frac{-1}{\Phi_1 - \Phi_1^*} \frac{\Phi_1 + a}{\Phi_1^* + a} & \frac{1}{-(\Phi_1 - \Phi_2) + \frac{\phi_2}{2}} \frac{\Phi_1 + a}{\Phi_1^* + a} & \frac{1}{-(\Phi_1 - \Phi_2^*) - \frac{\phi_2}{2}} \frac{\Phi_1 + a}{\Phi_1^* + a} \\ \frac{-1}{\Phi_1 - \Phi_1^*} \frac{\Phi_1^* + a}{\Phi_1 + a} & \omega_1^* + \frac{1}{\Phi_1^* + a} & \frac{1}{(\Phi_1^* - \Phi_2) - \frac{\phi_2}{2}} \frac{\Phi_1^* + a}{\Phi_1 + a} & \frac{1}{(\Phi_1^* - \Phi_2^*) + \frac{\phi_2}{2}} \frac{\Phi_1^* + a}{\Phi_1 + a} \\ \frac{1}{-(\Phi_2 - \Phi_1) + \frac{\phi_2}{2}} \frac{\phi_2 + a - \frac{\phi_2}{2}}{\Phi_1 + a} & \frac{1}{-(\Phi_2 - \Phi_1^*) + \frac{\phi_2}{2}} \frac{\phi_2 + a - \frac{\phi_2}{2}}{\Phi_1^* + a} & \frac{1}{\phi_2 \exp(\Psi_2)} + \frac{1}{\phi_2} \frac{\phi_2 + a - \frac{\phi_2}{2}}{\Phi_1 + a} & \frac{-1}{\Phi_2 - \Phi_2^*} \frac{\phi_2 + a - \frac{\phi_2}{2}}{\Phi_1 + a} \\ \frac{1}{(\Phi_2^* - \Phi_1) + \frac{\phi_2}{2}} \frac{\phi_2^* + a + \frac{\phi_2}{2}}{\Phi_1 + a} & \frac{1}{(\Phi_2^* - \Phi_1^*) + \frac{\phi_2}{2}} \frac{\phi_2^* + a + \frac{\phi_2}{2}}{\Phi_1^* + a} & \frac{-1}{\Phi_2 - \Phi_2^*} \frac{\phi_2^* + a + \frac{\phi_2}{2}}{\Phi_1 + a} & \frac{1}{\phi_2 \exp(\Psi_2^*)} + \frac{1}{\phi_2} \frac{\phi_2^* + a + \frac{\phi_2}{2}}{\Phi_1 + a} \end{vmatrix}
 \end{aligned} \tag{14}$$

where

$$\begin{aligned}
 \omega_1 &= ix + 2i\Phi_1 t - \frac{2i\varrho^2}{4\Phi_1^2} y, \\
 \Psi_2 &= i\phi_2 x + 2i\phi_2 \Phi_2 t - \frac{2i\phi_2 \varrho^2}{4\Phi_2^2 - \phi_2^2} y + \Psi_{2,0}
 \end{aligned}$$

Since the exp-solution involves two different cases, the breather and homoclinic orbit soliton, and the rational solution also involves two types, the lump solution and the rogue wave. Based on the permutation and combination rule, we know that the one-rational-one-exp solution will include four mixed types between exp-solution and rational solution. By choosing some proper parameters, we give the figures for the mixed type in Figures 11–14. It is easily to see that all of these solution will keep their own characters.

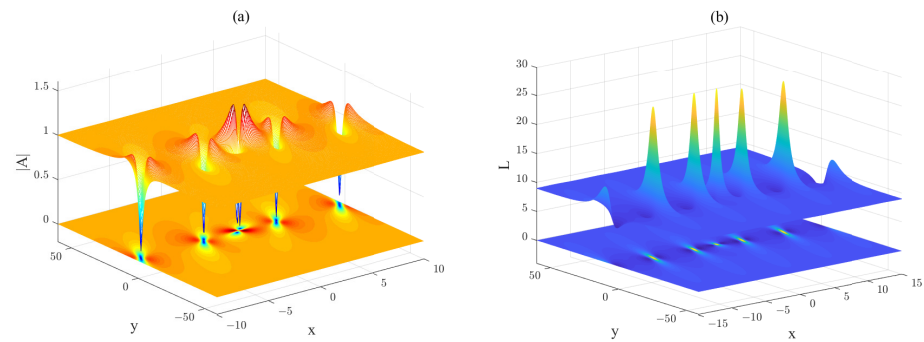


**Figure 11.** The interaction of lump solution and breather to Maccari system, the parameters are  $t = 0, a = 0, b = -10, \rho = 1, \Phi_{1R} = 1, \Phi_{1I} = 1, \Phi_{2R} = 2, \Phi_{2I} = 1, \phi_2 = 1, \Psi_{2,0} = 0$ : (a) short wave component  $A$ ; (b) long wave component  $L$ .

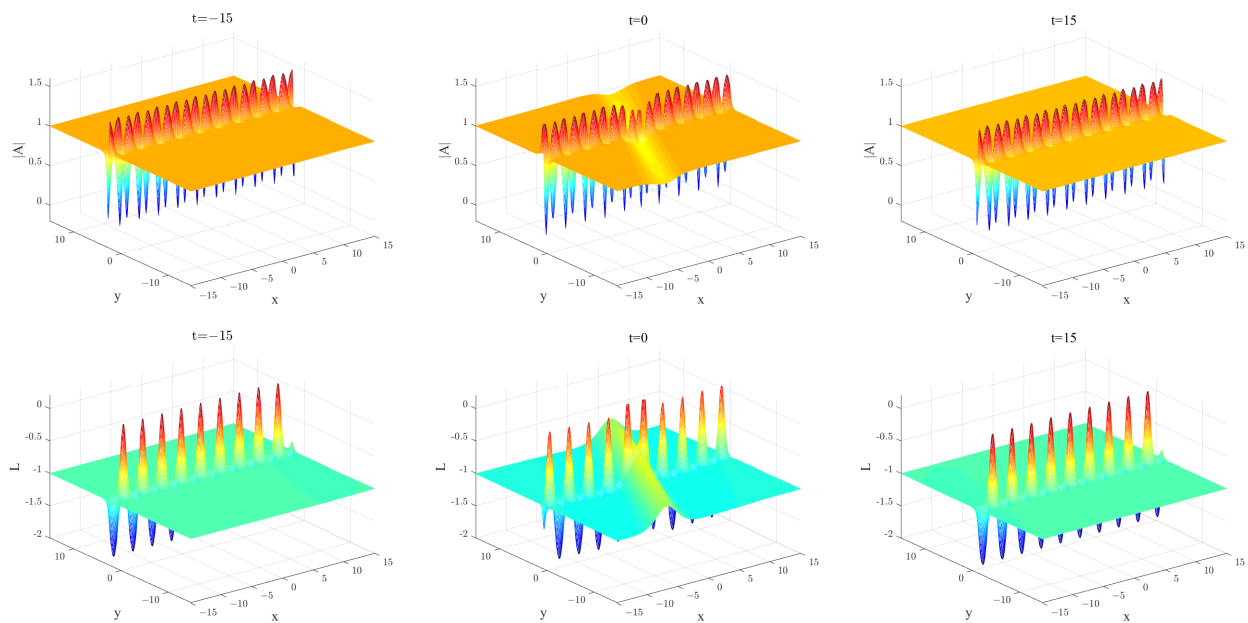


**Figure 12.** The evolution progress of breather and line rogue wave to Maccari system, the parameters are  $a = 0, b = 1, \rho = 1, \Phi_{1R} = -1, \Phi_{1I} = \frac{1}{6}, \Phi_{2R} = -1, \Phi_{2I} = \frac{1}{8}, \phi_2 = 2, \Psi_{2,0} = 0$ .

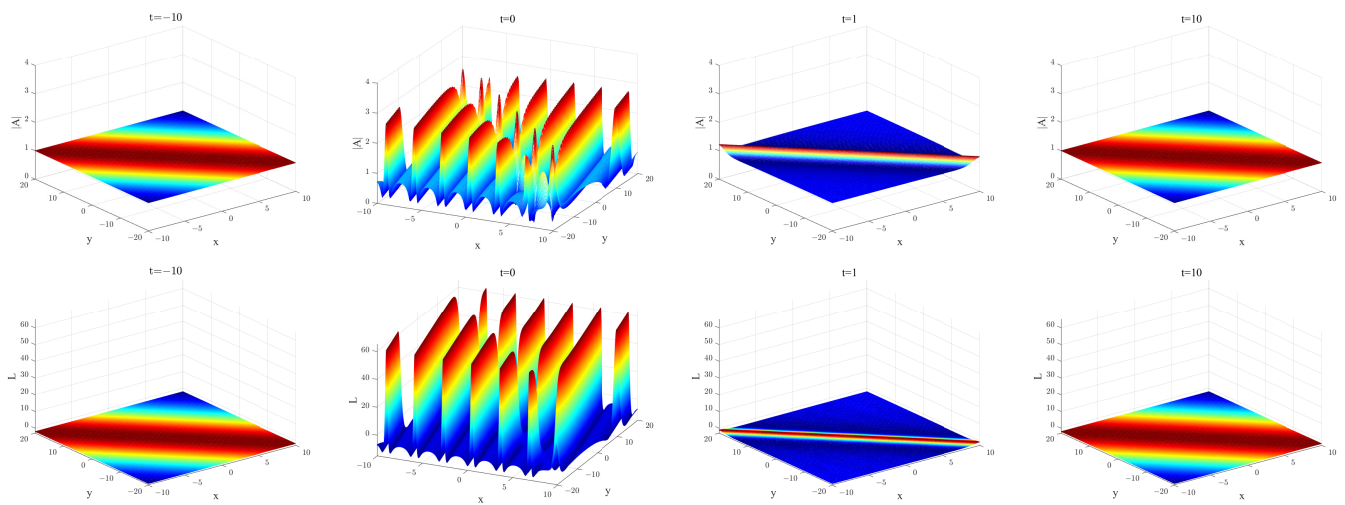


**Figure 13.** The evolution progress of homoclinic orbits and line rogue wave to Maccari system, the parameters are chosen as  $a = 0, b = 2, \rho = 1, \Phi_{1R} = 0, \Phi_{1I} = 1, \Phi_{2R} = 0, \Phi_{2I} = 2, \phi_2 = 2, \Psi_{2,0} = 0$ .

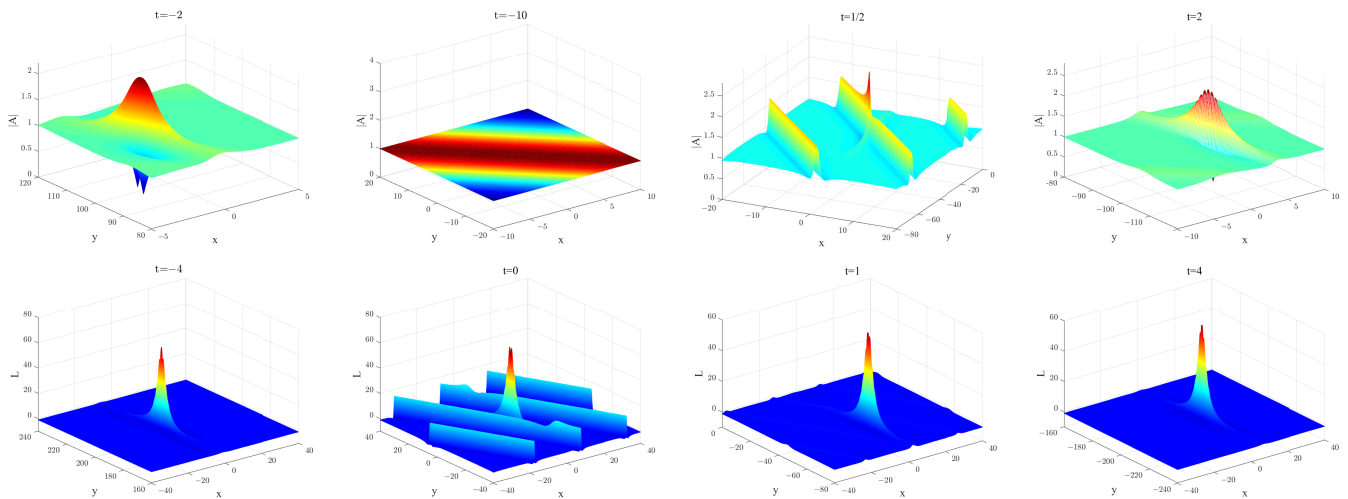


**Figure 14.** The evolution progress of lump soliton and homoclinic orbit to Maccari system by choosing  $a = 0, b = 1, \rho = 1, \Phi_{1R} = 1, \Phi_{1I} = 2, \Phi_{2R} = 0, \Phi_{2I} = 1, \phi_2 = \frac{1}{4}, \Psi_{2,0} = 0$ .

From these figures, we can see that the homoclinic orbits and the rogue wave have some common property, they all arise from the constant background, and they will appear at some time and then disappear. For both the long wave component  $L$  and short wave component  $A$ , the appearing time of rogue wave is longer than the homoclinic orbits. However, there are some differences, for example, the amplitude of rogue wave is higher than the homoclinic orbits to the short wave component  $A$ , but the long wave component  $L$  is inverse.

#### 4. Breather II

In Section 3, the choices to parameters  $\mu_{2k-1}, \mu_{2k}, \omega_{2k-1}, \omega_{2k}$  is Equation (A1), if taking  $\mu_{2k-1} \rightarrow i\mu_{2k-1}, \mu_{2k} \rightarrow -i\mu_{2k}, \omega_{2k-1} \rightarrow i\omega_{2k-1}, \omega_{2k} \rightarrow -i\omega_{2k}$ , we can get a quite different exp-solution. Compared to the homoclinic orbits, in this case, we get the dark-soliton or anti-dark soliton under some constraints. Meanwhile, the corresponding semi-rational solution will also be different.

Similar to the calculation in Appendix A, we give another Breather II in Appendix D. Still, we give the one breather by setting  $M = 1$  in Equation (A12), that is

$$\begin{aligned}
 A &= \frac{\varrho \exp(-ibt)g}{f}, \\
 u &= 2(\ln f)_{xx} - b, \\
 f &= 1 + \exp(\Psi_1) + \exp(\Psi_1^*) + A_{12} \exp(\Psi_1 + \Psi_1^*), \\
 g &= 1 + \frac{2i\Phi_1 + 2a - i\phi_1}{2i\Phi_1 + 2a + i\phi_1} \exp(\Psi_1) + \frac{2i\Phi_1^* - 2a + i\phi_1}{2i\Phi_1^* - 2a - i\phi_1} \exp(\Psi_1^*) \\
 &\quad + A_{12} \frac{2i\Phi_1 + 2a - i\phi_1}{2i\Phi_1 + 2a + i\phi_1} \frac{2i\Phi_1^* - 2a + i\phi_1}{2i\Phi_1^* - 2a - i\phi_1} \exp(\Psi_1 + \Psi_1^*)
 \end{aligned}$$

where

$$\begin{aligned}
 A_{12} &= \frac{-(\Phi_1^2 + \Phi_1^{*2})}{\phi_1^2 - (\Phi_1^2 + \Phi_1^{*2})}, \\
 \Psi_1 &= -\phi_1 x - 2i\phi_1 \Phi_1 t - \frac{2\phi_1 \varrho^2}{\phi_1^2 - 4\Phi_1^2} y + \Psi_{1,0}.
 \end{aligned}$$

Similarly, let  $\Phi_1 = \Phi_{1R} + i\Phi_{1I}$ , then  $\Psi_1 = \Psi_{1R} + i\Psi_{1I}$ , where

$$\begin{aligned}
 \Psi_{1R} &= \phi_1 \left[ 2\Phi_{1I} t - x - \frac{2\varrho^2(\phi_1^2 + 4\Phi_{1I}^2 - 4\Phi_{1R}^2)}{[4(\Phi_{1I}^2 - \Phi_{1R}^2) + \phi_1^2]^2 + 64\Phi_{1R}\Phi_{1I}} y \right] + \text{Re}(\Psi_{1,0}), \\
 \Psi_{1I} &= -2\phi_1 \Phi_{1R} \left[ t + \frac{8\varrho^2 \Phi_{1I}}{[4(\Phi_{1I}^2 - \Phi_{1R}^2) + \phi_1^2]^2 + 64\Phi_{1R}\Phi_{1I}} y \right] + \text{Im}(\Psi_{1,0}).
 \end{aligned}$$

From this exact expression, we can say that the breather II is similar to the breather I, but the periodicity and the localization behave quite differently, it present an opposite view. But moreover, we find some differences. In the first case,  $\Psi_{1I}$  involves two spatial variables  $x, y$  and one time variable  $t$ , while  $\Psi_{1R}$  involves one spatial variable  $y$  and one time variable  $t$ . Therefore, if the spatial variable  $y$  in  $\Psi_{1R}$  vanished, this breather will reduce to the homoclinic orbits. However, in this case, the dynamics is very different, that is,  $\Psi_{1R}$  involves two spatial variables and one time variable and  $\Psi_{1I}$  contains one spatial variable  $y$  and one time variable  $t$ . If  $\Psi_{1I}$  vanishes, this breather will reduce to the dark soliton or anti-dark solution. Next, we give Figures 15 and 16 to present this dynamics clearly reduced into dark soliton or anti-dark soliton.

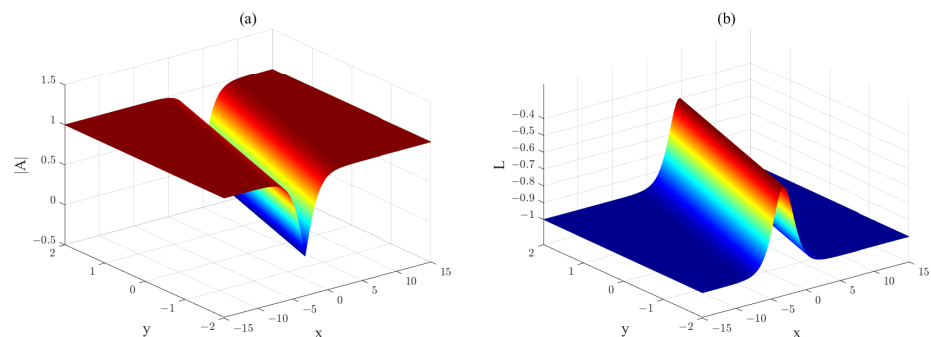


**Figure 15.** Dark soliton to Maccari system at  $t = 0$ , the corresponding parameters are  $a = 0$ ,  $b = 1, \varrho = 1, \Phi_{1R} = 0, \Phi_{1I} = 0, \phi_1 = 1, \Psi_{1,0} = 0$ : (a) short wave component  $A$ ; (b) long wave component  $L$ .

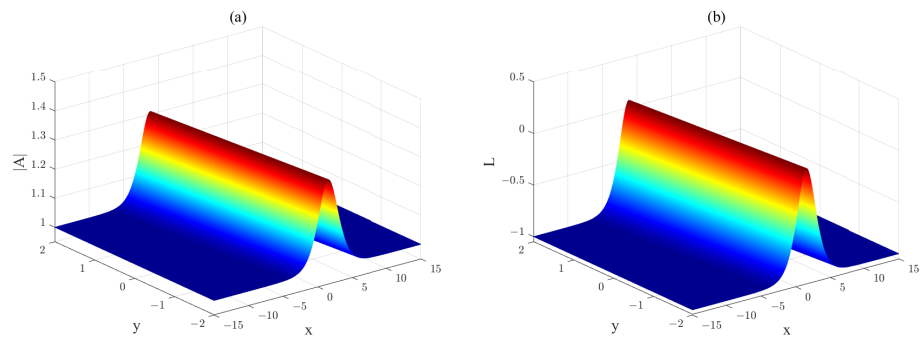


**Figure 16.** Anti-dark soliton to Maccari system at  $t = 0$ , the parameters are  $a = 0, b = 1, \rho = 1, \Phi_{1R} = 1, \Phi_{1I} = 0, \phi_1 = 1, \Psi_{1,0} = 0$ : **(a)** short wave component  $A$ ; **(b)** long wave component  $L$ .

In Figure 15, we give the dark soliton by choosing  $a = 0, b = 1, \rho = 1, \Phi_{1R} = 0, \Phi_{1I} = 0, \phi_1 = 1, \Psi_{1,0} = 0, t = 0$ , then the corresponding solution of  $|A|$  is

$$|A| = \left| \frac{2e^{-x+2y} - 1}{2e^{-x+2y} + 1} \right|,$$

obviously,  $|A|$  is equal to zero along the line  $-x + 2y = -\ln(2)$ . When  $-x + 2y \rightarrow \pm\infty, |A| \rightarrow 1$ , thus we see  $A$  is a dark soliton. While Figure 16 is the anti-dark soliton by choosing  $a = 0, b = 1, \rho = 1, \Phi_{1R} = 1, \Phi_{1I} = 0, \phi_1 = 1, \Psi_{1,0} = 0$ , then the corresponding  $|A|$  is

$$|A| = \left| \frac{4e^{-2x-\frac{4}{3}y} + 10e^{-x-\frac{2}{3}y} + 3}{4e^{-2x-\frac{4}{3}y} + 6e^{-x-\frac{2}{3}y} + 3} \right|$$

$$\frac{\partial|A|}{\partial x} = \left| \frac{4e^{-x-\frac{2y}{3}} \left( 4e^{-2x-\frac{4y}{3}} - 3 \right)}{\left( 4e^{-2x-\frac{4}{3}y} + 6e^{-x-\frac{2}{3}y} + 3 \right)^2} \right|, \quad \frac{\partial|A|}{\partial y} = \left| \frac{8}{3} \frac{e^{-x-\frac{2y}{3}} \left( 4e^{-2x-\frac{4y}{3}} - 3 \right)}{\left( 4e^{-2x-\frac{4}{3}y} + 6e^{-x-\frac{2}{3}y} + 3 \right)^2} \right|.$$

By a direct calculation, we know that the maximum of  $|A|$  is  $\frac{6+5\sqrt{3}}{3(2+\sqrt{3})} > 1$  along the line  $(-x - \frac{2}{3}y) = \ln(\frac{\sqrt{3}}{2})$ . And when  $(-x - \frac{2}{3}y) \rightarrow \pm\infty$ , we have  $|A| \rightarrow 1$ , thus we call it the anti-dark soliton.

Furthermore, we also present the interactions for the two-breather in Figures 17–21. From the characters of one-breather, we know that the dynamics of the second-breather in this case becomes more diverse. It not only contains the same kind of wave but also two different kinds of waves. For the mixed waves, we only give two different cases, the breather and dark soliton, dark soliton and anti-dark soliton, others are omitted. From these figures, we find an interesting phenomenon, compared to the breather, the amplitude of the soliton is much smaller, so the soliton is inconspicuous. Moreover, for the two-breather case, the dynamics in this case is different from the first case, one is two parallel breathers and the other one is inter-sectional types.

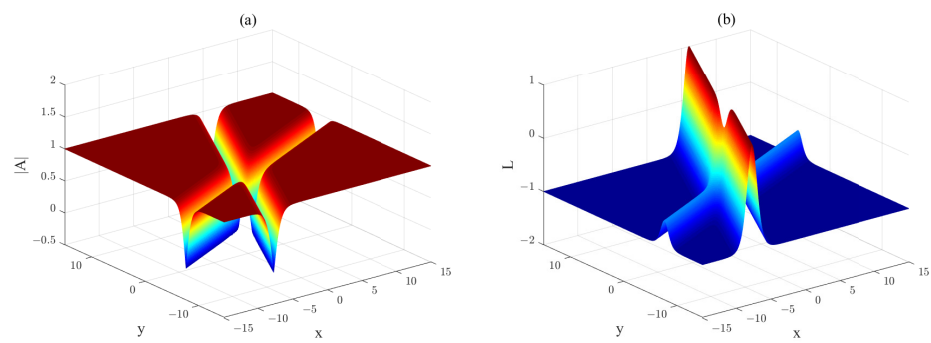


**Figure 17.** Two dark solitons to Maccari system with the parameters  $t = 0, a = 0, b = 1, \rho = 1, \Phi_{1R} = 0, \phi_1 = 0, \Phi_{1I} = 1, \Phi_{2R} = 0, \Phi_{2I} = 0, \phi_2 = -2, \Psi_{1,0} = 0, \Psi_{2,0} = 0$ : (a) short wave component  $A$ ; (b) long wave component  $L$ .

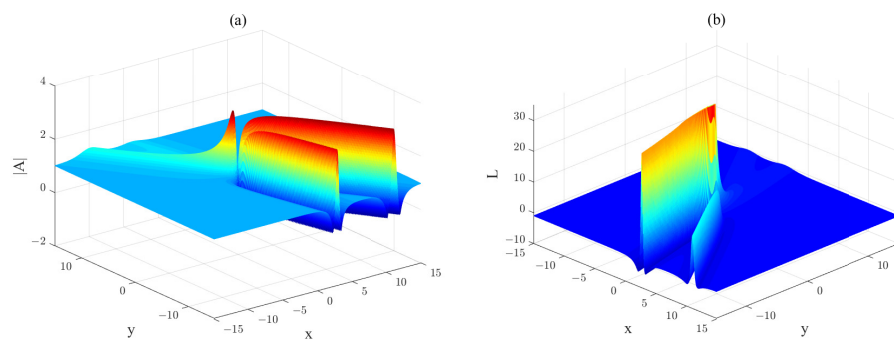


**Figure 18.** Two anti-dark solitons to Maccari system by choosing  $t = 0, a = 0, b = 1, \rho = 1, \Phi_{1R} = 1, \phi_1 = 1, \Phi_{1I} = 0, \Phi_{2R} = \frac{3}{2}, \Phi_{2I} = 0, \phi_2 = -1, \Psi_{1,0} = 0, \Psi_{2,0} = 0$ : (a) short wave component  $A$ ; (b) long wave component  $L$ .

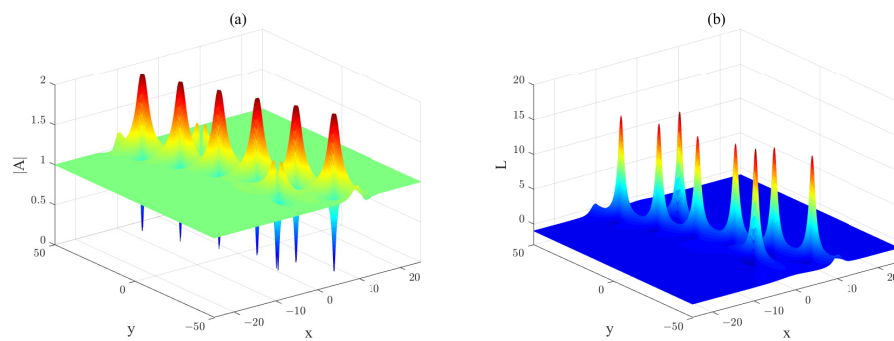


**Figure 19.** Two breathers to Maccari system at  $t = 0$  by choosing  $a = 0, b = 1, \rho = 1, \Phi_{1R} = 0, \phi_1 = 1, \Phi_{1I} = 0, \Phi_{2R} = 1, \Phi_{2I} = 0, \phi_2 = -1, \Psi_{1,0} = 0, \Psi_{2,0} = 0$ : (a) short wave component  $A$ ; (b) long wave component  $L$ .

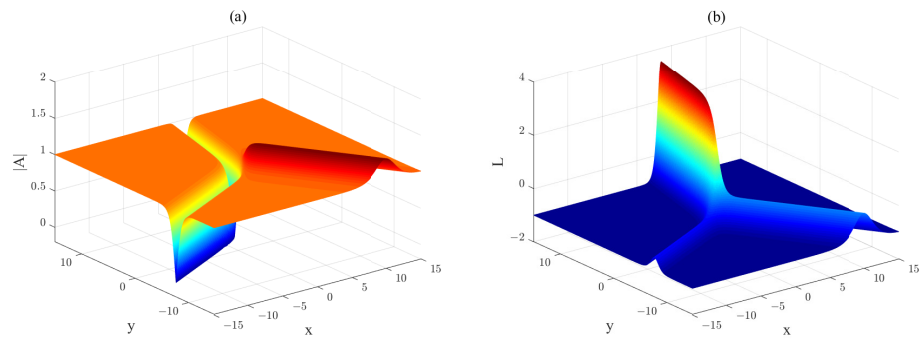


**Figure 20.** The interaction of dark soliton and anti-dark soliton to Maccari system, the corresponding parameters are  $t = 0, a = 0, b = 1, \rho = 1, \Phi_{1R} = 1, \phi_1 = 1, \Phi_{1I} = -1, \Phi_{2R} = 0, \Phi_{2I} = 1, \phi_2 = 1, \Psi_{1,0} = 0, \Psi_{2,0} = 0$ : (a) short wave component  $A$ ; (b) long wave component  $L$ .

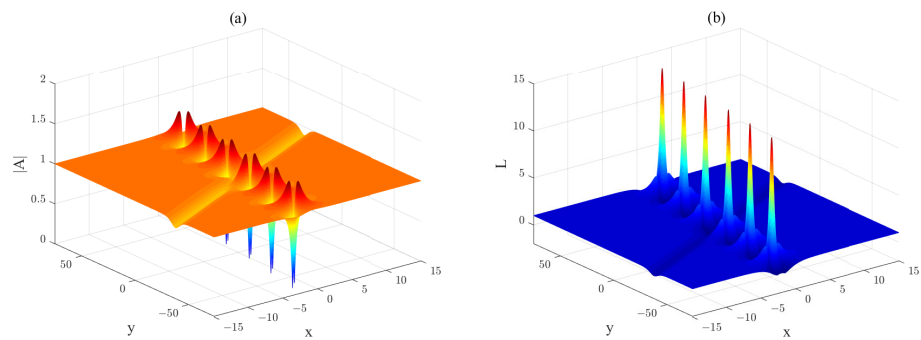


**Figure 21.** The interaction between dark soliton and general breather to Maccari system, the corresponding parameters are  $t = 0, a = 0, b = 1, \rho = 1, \Phi_{1R} = 1, \phi_1 = 1, \Phi_{1I} = -1, \Phi_{2R} = 0, \Phi_{2I} = 1, \phi_2 = 1, \Psi_{1,0} = 0, \Psi_{2,0} = 0$ : (a) short wave component  $A$ ; (b) long wave component  $L$ .

Similar to the first breather, we can also construct the rational solution basing on the same limiting skill. By a simple calculation, we give the rational solution to Maccari system,

$$\begin{aligned}
 A &= \frac{\rho \exp(-ibt)g}{f}, \\
 u &= 2(\ln f)_{xx} - b,
 \end{aligned}
 \tag{15}$$

where  $f = |F_{k,l}|, g = |G_{k,l}|$ , the entries of these matrices are as follows:

$$\begin{aligned}
 F_{k,k} &= \begin{bmatrix} \omega_k & \frac{i}{\Phi_k + \Phi_k^*} \\ \frac{i}{\Phi_k + \Phi_k^*} & \omega_k^* \end{bmatrix} \\
 G_{k,k} &= \begin{bmatrix} \omega_k - \frac{1}{i\Phi_k + a} & \frac{i}{\Phi_k + \Phi_k^*} \frac{-\Phi_k + ia}{\Phi_k^* + ia} \\ \frac{i}{\Phi_k + \Phi_k^*} \frac{-\Phi_k^* - ia}{\Phi_k - ia} & \omega_k^* - \frac{1}{i\Phi_k^* - a} \end{bmatrix} \\
 F_{k,l} &= \begin{bmatrix} \frac{i}{\Phi_k - \Phi_l} & \frac{i}{\Phi_k + \Phi_l^*} \\ \frac{i}{\Phi_k^* + \Phi_l} & \frac{i}{\Phi_k^* - \Phi_l^*} \end{bmatrix} \\
 G_{k,l} &= \begin{bmatrix} \frac{i}{\Phi_k - \Phi_l} \frac{i\Phi_k + a}{i\Phi_l + a} & \frac{i}{\Phi_k + \Phi_l^*} \frac{i\Phi_k + a}{-i\Phi_l^* + a} \\ \frac{i}{\Phi_k^* - \Phi_l} \frac{-i\Phi_k^* + a}{i\Phi_l + a} & \frac{i}{\Phi_k^* - \Phi_l^*} \frac{i}{-i\Phi_l^* + a} \end{bmatrix}
 \end{aligned}
 \tag{16}$$

where

$$\omega_k = ix - 2\Phi_k t + \frac{2i\varrho^2}{4\Phi_k^2} y.$$

Since the rational solutions are given with the same skill, so their expressions and the dynamics are also the same as the first case, we do not give it anymore.

Although the rational solutions are the same, the breathers in the second case are different from the first case, thus the semi-rational solution will also be different. The detailed calculations are given in Appendix E. By setting  $\tilde{N} = \hat{N} = 1$  in Equation (A14), we get the semi-rational solution as

$$\begin{aligned}
 A &= \frac{\varrho \exp(-ibt)g}{f}, \\
 u &= 2(\ln(\exp(\Psi_2 + \Psi_2^*)\phi_2^2) \cdot f)_{xx} - b, \\
 f &= \begin{vmatrix} \omega_1 & \frac{i}{\Phi_1 + \Phi_1^*} & \frac{i}{\Phi_1 - \Phi_2 - \frac{\phi_2}{2}} & \frac{i}{\Phi_1 + \Phi_2^* - \frac{\phi_2}{2}} \\ \frac{i}{\Phi_1 + \Phi_1^*} & \omega_1^* & \frac{i}{(\Phi_1^* + \Phi_2) + \frac{\phi_2}{2}} & \frac{i}{(\Phi_1^* - \Phi_2^*) + \frac{\phi_2}{2}} \\ \frac{i}{\Phi_2 - \Phi_1 - \frac{\phi_2}{2}} & \frac{i}{\Phi_2 + \Phi_1^* - \frac{\phi_2}{2}} & \frac{-i}{\phi_2 \exp(\Psi_2)} + \frac{-i}{\phi_2} & \frac{i}{\Phi_2 + \Phi_2^* - \phi_2} \\ \frac{i}{(\Phi_2^* + \Phi_1) + \frac{\phi_2}{2}} & \frac{i}{(\Phi_2^* - \Phi_1^*) + \frac{\phi_2}{2}} & \frac{i}{\Phi_2 + \Phi_2^* + \phi_2} & \frac{i}{\phi_2 \exp(\Psi_2^*)} + \frac{i}{\phi_2} \end{vmatrix}, \\
 g &= \begin{vmatrix} \omega_1 - \frac{1}{i\Phi_1 + a} & \frac{i}{\Phi_1 + \Phi_1^*} \frac{-\Phi_1 + ia}{\Phi_1^* + ia} & \frac{i}{\Phi_1 - \Phi_2 - \frac{\phi_2}{2}} \frac{\Phi_1 - ia}{\Phi_2 - ia + \frac{\phi_2}{2}} & \frac{i}{\Phi_1 + \Phi_2^* - \frac{\phi_2}{2}} \frac{\Phi_1 - ia}{-\Phi_2^* - ia + \frac{\phi_2}{2}} \\ \frac{i}{\Phi_1 + \Phi_1^*} \frac{-\Phi_1^* - ia}{\Phi_1 - ia} & \omega_1^* - \frac{1}{i\Phi_1^* - a} & \frac{i}{(\Phi_1^* + \Phi_2) + \frac{\phi_2}{2}} \frac{-\Phi_2 + ia - \frac{\phi_2}{2}}{-\Phi_2 + ia - \frac{\phi_2}{2}} & \frac{i}{(\Phi_1^* - \Phi_2^*) + \frac{\phi_2}{2}} \frac{\Phi_2^* + ia - \frac{\phi_2}{2}}{\Phi_2^* + ia - \frac{\phi_2}{2}} \\ \frac{i}{\Phi_2 - \Phi_1 - \frac{\phi_2}{2}} \frac{\Phi_2 - ia - \frac{\phi_2}{2}}{\Phi_1 - ia} & \frac{i}{\Phi_2 + \Phi_1^* - \frac{\phi_2}{2}} \frac{\Phi_2 - ia - \frac{\phi_2}{2}}{-\Phi_1^* - ia} & \frac{-i}{\phi_2 \exp(\Psi_2)} + \frac{-i}{\phi_2} \frac{\Phi_2 - ia - \frac{\phi_2}{2}}{\Phi_2 - ia + \frac{\phi_2}{2}} & \frac{i}{\Phi_2 + \Phi_2^* - \phi_2} \frac{\Phi_2 - ia - \frac{\phi_2}{2}}{-\Phi_2^* - ia + \frac{\phi_2}{2}} \\ \frac{i}{(\Phi_2^* + \Phi_1) + \frac{\phi_2}{2}} \frac{\Phi_2^* + ia + \frac{\phi_2}{2}}{-\Phi_1 + ia} & \frac{i}{(\Phi_2^* - \Phi_1^*) + \frac{\phi_2}{2}} \frac{\Phi_2^* + ia + \frac{\phi_2}{2}}{\Phi_1^* + ia} & \frac{i}{\Phi_2 + \Phi_2^* + \phi_2} \frac{\Phi_2^* + ia + \frac{\phi_2}{2}}{-\Phi_2 + ia - \frac{\phi_2}{2}} & \frac{i}{\phi_2 \exp(\Psi_2^*)} + \frac{i}{\phi_2} \frac{\Phi_2^* + ia + \frac{\phi_2}{2}}{\Phi_2^* + ia - \frac{\phi_2}{2}} \end{vmatrix}
 \end{aligned} \tag{17}$$

with

$$\begin{aligned}
 \omega_1 &= ix - 2\Phi_1 t + \frac{2i\varrho^2}{4\Phi_1^2} y, \\
 \Psi_2 &= -\phi_2 x - 2i\phi_2 \Phi_2 t - \frac{2\phi_2 \varrho^2}{\phi_2^2 - 4\Phi_2^2} y + \Psi_{2,0}.
 \end{aligned}$$

It is easily to see that the semi-rational solutions will involve six types, one is from one kind of these three different breathers and the other one is from one of the two kinds of rational solutions. Here, we only give two examples to describe the semi-rational solutions, which are shown in Figures 22 and 23.

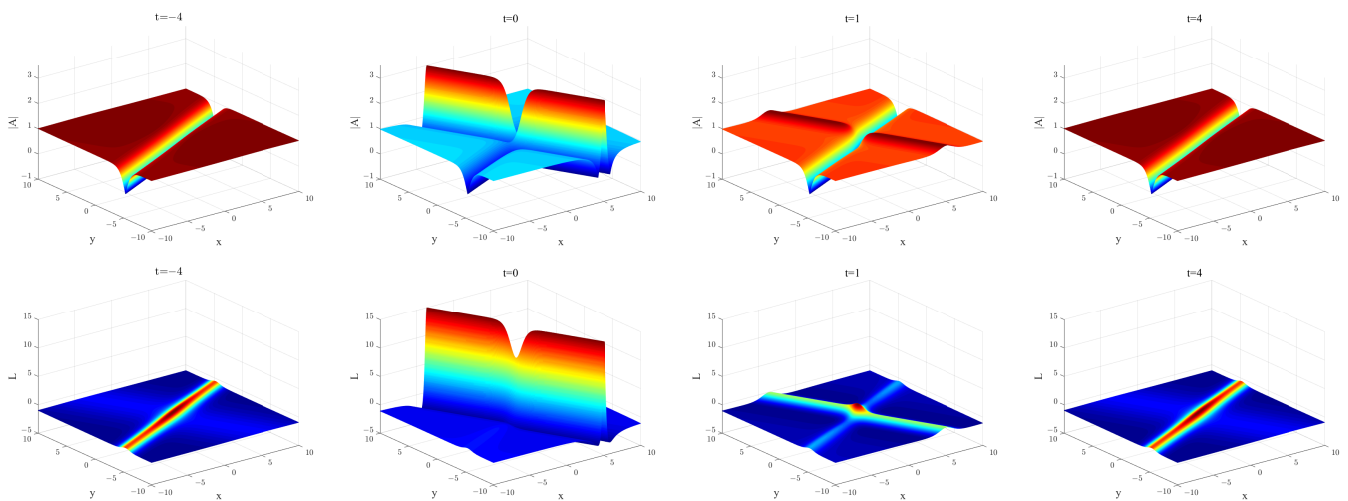


**Figure 22.** The evolution progress of dark soliton and line rogue wave, the parameters are chosen as  $a = 0, b = 1, \rho = 1, \Phi_{1R} = 1, \Phi_{1I} = -1, \Phi_{2R} = 0, \Phi_{2I} = 1, \phi_2 = 1, \Psi_{2,0} = 0$ .

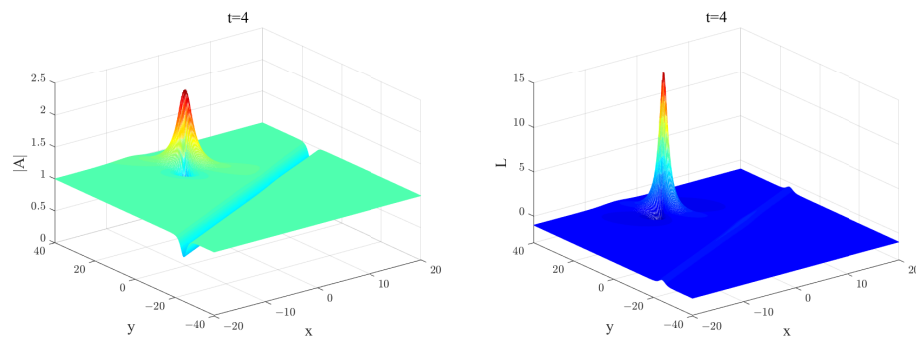


**Figure 23.** The semi-rational solution of dark soliton and lump soliton at a fixed time  $t = 4$ , the other parameters are  $a = 0, b = 1, \rho = 1, \Phi_{1R} = 1, \Phi_{1I} = \frac{1}{2}, \Phi_{2R} = 0, \Phi_{2I} = \frac{1}{2}, \phi_2 = 1, \Psi_{2,0} = 0$ .

In this case, the dynamics of breather is very attracting, thus we also give the interactions between two kinds of breather and one kind of rational solution, the corresponding exact expression is given as

$$\begin{aligned}
 A &= \frac{\rho \exp(-ibt)g}{f}, \\
 u &= 2(\ln(\exp(\Psi_2 + \Psi_2^* + \Psi_3 + \Psi_3^*)\phi_2^2\phi_3^2) \cdot f)_{xx} - b,
 \end{aligned}
 \tag{18}$$

$$\begin{aligned}
 f = & \left( \begin{array}{cccccc}
 \frac{\omega_1}{\Phi_1 + \Phi_1^*} & \frac{i}{\Phi_1 + \Phi_1^*} & \frac{i}{\Phi_1 - \Phi_2 - \frac{\phi_2}{2}} & \frac{i}{\Phi_1 + \Phi_2^* - \frac{\phi_2}{2}} & \frac{i}{\Phi_1 - \Phi_3 - \frac{\phi_3}{2}} & \frac{i}{\Phi_1 + \Phi_3^* - \frac{\phi_3}{2}} \\
 \frac{i}{\Phi_2 - \Phi_1 - \frac{\phi_2}{2}} & \frac{\omega_1^*}{\Phi_2 + \Phi_1^* - \frac{\phi_2}{2}} & \frac{i}{(\Phi_1^* + \Phi_2) + \frac{\phi_2}{2}} & \frac{i}{(\Phi_1^* - \Phi_2^*) + \frac{\phi_2}{2}} & \frac{i}{(\Phi_1^* + \Phi_3) + \frac{\phi_3}{2}} & \frac{i}{(\Phi_1^* - \Phi_3^*) + \frac{\phi_3}{2}} \\
 \frac{i}{(\Phi_2^* + \Phi_1) + \frac{\phi_2}{2}} & \frac{i}{(\Phi_2^* - \Phi_1^*) + \frac{\phi_2}{2}} & \frac{-i}{\phi_2 \exp(\Psi_2) + \frac{-i}{\phi_2}} & \frac{i}{\Phi_2 + \Phi_2^* - \phi_2} & \frac{i}{\Phi_2 - \Phi_3 - \frac{\phi_2 + \phi_3}{2}} & \frac{i}{\Phi_2 + \Phi_3^* - \frac{\phi_2 + \phi_3}{2}} \\
 \frac{i}{\Phi_3 - \Phi_1 - \frac{\phi_3}{2}} & \frac{i}{\Phi_1^* + \Phi_3 - \frac{\phi_3}{2}} & \frac{i}{\Phi_2 + \Phi_2^* + \phi_2} & \frac{i}{\phi_2 \exp(\Psi_2^*) + \frac{i}{\phi_2}} & \frac{i}{\Phi_2^* + \Phi_3 + \frac{\phi_2 + \phi_3}{2}} & \frac{i}{\Phi_2^* - \Phi_3^* + \frac{\phi_2 + \phi_3}{2}} \\
 \frac{i}{\Phi_3^* + \Phi_1 + \frac{\phi_3}{2}} & \frac{i}{\Phi_3^* - \Phi_1^* + \frac{\phi_3}{2}} & \frac{i}{\Phi_3 + \Phi_2 + \frac{\phi_2 + \phi_3}{2}} & \frac{i}{\Phi_3 + \Phi_2^* - \frac{\phi_2 + \phi_3}{2}} & \frac{-i}{\phi_2 \exp(\Psi_3) + \frac{-i}{\phi_3}} & \frac{i}{\Phi_2 + \Phi_2^* - \phi_3} \\
 \frac{i}{\Phi_3^* + \Phi_1 + \frac{\phi_3}{2}} & \frac{i}{\Phi_3^* - \Phi_1^* + \frac{\phi_3}{2}} & \frac{i}{\Phi_3 + \Phi_2 + \frac{\phi_2 + \phi_3}{2}} & \frac{i}{\Phi_3^* - \Phi_2^* + \frac{\phi_2 + \phi_3}{2}} & \frac{i}{\Phi_3 + \Phi_3^* + \phi_3} & \frac{i}{\phi_3 \exp(\Psi_3^*) + \frac{i}{\phi_3}}
 \end{array} \right), \\
 g = & \left( \begin{array}{cccccc}
 \omega_1 - \frac{1}{i\Phi_1 + a} & \frac{i}{\Phi_1 + \Phi_1^*} & \frac{-\Phi_1 + ia}{\Phi_1 + ia} & \frac{i}{\Phi_1 - \Phi_2 - \frac{\phi_2}{2}} & \frac{\Phi_1 - ia}{\Phi_2 - ia + \frac{\phi_2}{2}} & \frac{i}{\Phi_1 + \Phi_2^* - \frac{\phi_2}{2}} & \frac{\Phi_1 - ia}{-\Phi_2^* - ia + \frac{\phi_2}{2}} & \mathcal{G}_{15} & \mathcal{G}_{16} \\
 \frac{i}{\Phi_1 + \Phi_1^*} & \frac{-\Phi_1^* - ia}{\Phi_1 - ia} & \omega_1^* - \frac{1}{i\Phi_1^* - a} & \frac{i}{\Phi_2 + \Phi_1^* - \frac{\phi_2}{2}} & \frac{\Phi_1^* + ia}{-\Phi_2 + ia - \frac{\phi_2}{2}} & \frac{i}{(\Phi_1^* - \Phi_2^*) + \frac{\phi_2}{2}} & \frac{\Phi_1^* + ia}{\Phi_2^* + ia - \frac{\phi_2}{2}} & \mathcal{G}_{25} & \mathcal{G}_{26} \\
 \frac{i}{\Phi_2 - \Phi_1 - \frac{\phi_2}{2}} & \frac{\Phi_2 - ia - \frac{\phi_2}{2}}{\Phi_1 - ia} & \frac{i}{\Phi_2 + \Phi_1^* - \frac{\phi_2}{2}} & \frac{\Phi_2 - ia - \frac{\phi_2}{2}}{-\Phi_1^* - ia} & \frac{-i}{\phi_2 \exp(\Psi_2) + \frac{-i}{\phi_2}} & \frac{-i}{\phi_2} & \frac{\Phi_2 - ia - \frac{\phi_2}{2}}{\Phi_2 - ia + \frac{\phi_2}{2}} & \mathcal{G}_{35} & \mathcal{G}_{36} \\
 \frac{i}{(\Phi_2^* + \Phi_1) + \frac{\phi_2}{2}} & \frac{\Phi_2^* + ia + \frac{\phi_2}{2}}{-\Phi_1 + ia} & \frac{i}{(\Phi_2^* - \Phi_1^*) + \frac{\phi_2}{2}} & \frac{\Phi_2^* + ia + \frac{\phi_2}{2}}{\Phi_1^* + ia} & \frac{i}{\Phi_2 + \Phi_2^* + \phi_2} & \frac{\Phi_2^* + ia + \frac{\phi_2}{2}}{-\Phi_2 + ia - \frac{\phi_2}{2}} & \frac{i}{\phi_2 \exp(\Psi_2^*) + \frac{i}{\phi_2}} & \frac{\Phi_2^* + ia + \frac{\phi_2}{2}}{\Phi_2^* + ia - \frac{\phi_2}{2}} & \mathcal{G}_{45} & \mathcal{G}_{46} \\
 \frac{i}{(\Phi_3^* + \Phi_1) + \frac{\phi_3}{2}} & \frac{\Phi_3^* + ia + \frac{\phi_3}{2}}{-\Phi_1 + ia} & \frac{i}{(\Phi_3^* - \Phi_1^*) + \frac{\phi_3}{2}} & \frac{\Phi_3^* + ia + \frac{\phi_3}{2}}{\Phi_1^* + ia} & \frac{i}{\Phi_3 - \Phi_2 - \frac{\phi_2 + \phi_3}{2}} & \frac{\Phi_3 - ia - \frac{\phi_3}{2}}{\Phi_2 - ia + \frac{\phi_2}{2}} & \frac{i}{\Phi_3 + \Phi_2^* - \frac{\phi_2 + \phi_3}{2}} & \frac{\Phi_3 - ia - \frac{\phi_3}{2}}{-\Phi_2^* - ia + \frac{\phi_2}{2}} & \mathcal{G}_{55} & \mathcal{G}_{56} \\
 \frac{i}{(\Phi_3^* + \Phi_1) + \frac{\phi_3}{2}} & \frac{\Phi_3^* + ia + \frac{\phi_3}{2}}{-\Phi_1 + ia} & \frac{i}{(\Phi_3^* - \Phi_1^*) + \frac{\phi_3}{2}} & \frac{\Phi_3^* + ia + \frac{\phi_3}{2}}{\Phi_1^* + ia} & \frac{i}{\Phi_3 + \Phi_2 + \frac{\phi_2 + \phi_3}{2}} & \frac{\Phi_3^* + ia + \frac{\phi_3}{2}}{-\Phi_2 + ia - \frac{\phi_2}{2}} & \frac{i}{\Phi_3^* - \Phi_2^* + \frac{\phi_2 + \phi_3}{2}} & \frac{\Phi_3^* + ia + \frac{\phi_3}{2}}{\Phi_2^* + ia - \frac{\phi_2}{2}} & \mathcal{G}_{65} & \mathcal{G}_{66}
 \end{array} \right), \\
 & \text{where}
 \end{aligned}
 \tag{19}$$

$$\begin{aligned}
 \mathcal{G}_{15} &= \frac{i}{\Phi_1 - \Phi_3 - \frac{\phi_3}{2}} \frac{\Phi_1 - ia}{\Phi_3 - ia + \frac{\phi_3}{2}} \\
 \mathcal{G}_{16} &= \frac{i}{\Phi_1 + \Phi_3^* - \frac{\phi_3}{2}} \frac{\Phi_1 - ia}{-\Phi_3^* - ia + \frac{\phi_3}{2}} \\
 \mathcal{G}_{25} &= \frac{i}{(\Phi_1^* + \Phi_3) + \frac{\phi_3}{2}} \frac{\Phi_1^* + ia}{-\Phi_3 + ia - \frac{\phi_3}{2}} \\
 \mathcal{G}_{26} &= \frac{i}{(\Phi_1^* - \Phi_3^*) + \frac{\phi_3}{2}} \frac{\Phi_1^* + ia}{\Phi_3^* + ia - \frac{\phi_3}{2}} \\
 \mathcal{G}_{35} &= \frac{i}{\Phi_2 - \Phi_3 - \frac{\phi_2 + \phi_3}{2}} \frac{\Phi_2 - ia - \frac{\phi_2}{2}}{\Phi_3 - ia + \frac{\phi_2}{2}} \\
 \mathcal{G}_{36} &= \frac{i}{\Phi_2 + \Phi_3^* - \frac{\phi_2 + \phi_3}{2}} \frac{\Phi_2 - ia - \frac{\phi_2}{2}}{-\Phi_3^* - ia + \frac{\phi_2}{2}} \\
 \mathcal{G}_{45} &= \frac{i}{\Phi_2^* + \Phi_3 + \frac{\phi_2 + \phi_3}{2}} \frac{\Phi_2^* + ia + \frac{\phi_2}{2}}{-\Phi_3 + ia - \frac{\phi_3}{2}} \\
 \mathcal{G}_{46} &= \frac{i}{\Phi_2^* - \Phi_3^* + \frac{\phi_2 + \phi_3}{2}} \frac{\Phi_2^* + ia + \frac{\phi_2}{2}}{\Phi_3^* + ia - \frac{\phi_3}{2}} \\
 \mathcal{G}_{55} &= \frac{-i}{\phi_3 \exp(\Psi_3)} + \frac{-i}{\phi_3} \frac{\Phi_3 - ia - \frac{\phi_3}{2}}{\Phi_3 - ia + \frac{\phi_3}{2}} \\
 \mathcal{G}_{56} &= \frac{i}{\Phi_3 + \Phi_3^* - \phi_3} \frac{\Phi_3 - ia - \frac{\phi_3}{2}}{-\Phi_3^* - ia + \frac{\phi_3}{2}} \\
 \mathcal{G}_{65} &= \frac{i}{\Phi_3 + \Phi_3^* + \phi_3} \frac{\Phi_3^* + ia + \frac{\phi_3}{2}}{-\Phi_3 + ia - \frac{\phi_3}{2}}
 \end{aligned}$$

$$g_{66} = \frac{i}{\phi_3 \exp(\Psi_3^*)} + \frac{i}{\phi_3} \frac{\Phi_3^* + ia + \frac{\phi_3}{2}}{\Phi_3^* + ia - \frac{\phi_3}{2}}$$

$$\omega_1 = ix - 2\Phi_1 t + \frac{2i\phi_1^2}{4\Phi_1^2} y,$$

$$\Psi_2 = -\phi_2 x - 2i\phi_2 \Phi_2 t - \frac{2\phi_2 \phi_2^2}{\phi_2^2 - 4\Phi_2^2} y + \Psi_{2,0},$$

$$\Psi_3 = -\phi_3 x - 2i\phi_3 \Phi_3 t - \frac{2\phi_3 \phi_3^2}{\phi_3^2 - 4\Phi_3^2} y + \Psi_{3,0}.$$

As the dynamics for this case becomes richer, we only give one example composed by the breather, dark soliton and rogue wave in Figure 24

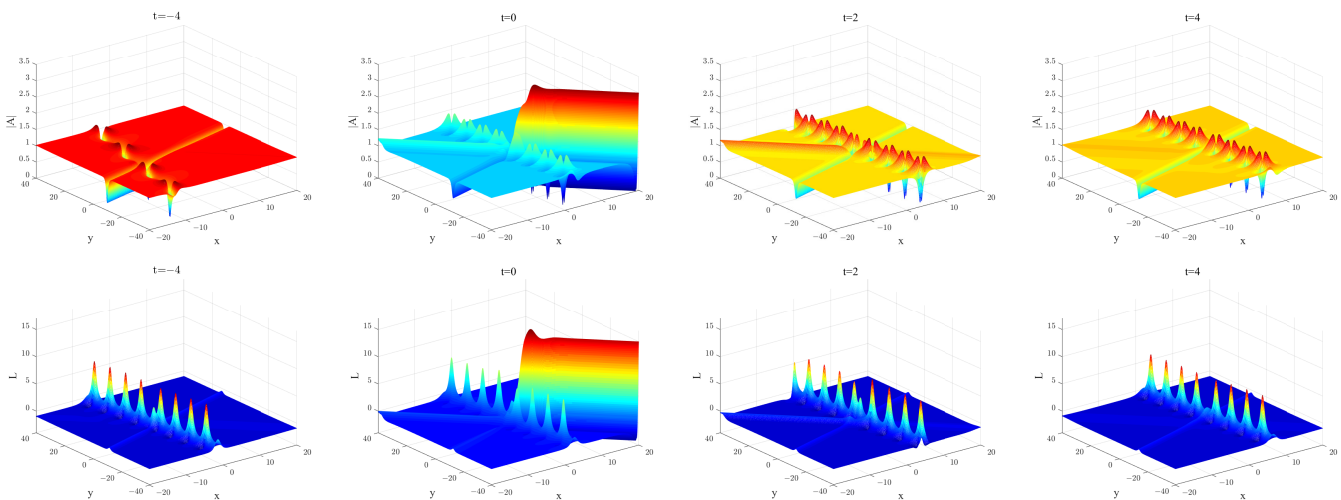


**Figure 24.** The evolution progress of three states, the parameters are  $a = 0, b = 1, \phi = 1, \Phi_{1R} = 1, \Phi_{1I} = 0, \Phi_{2R} = \frac{3}{4}, \Phi_{2I} = \frac{1}{2}, \phi_2 = 1, \Phi_{3R} = 0, \Phi_{3I} = \frac{1}{4}, \phi_3 = 1, \Psi_{2,0} = 0, \Psi_{3,0} = 0$ .

This evolution progress is very supernatural. The dark soliton and the breather exist all the time, they are crossed each other in the beginning. When the rogue wave appears, it is affected by the dark soliton and the breather heavily. A typical feature can be seen from the variation of amplitude. The amplitude of one half of the wave was significantly higher than that of the other. Thus we can say that the energy of rogue wave will be weakened by the dark soliton and the breather. As time moves, the amplitude of rogue wave will reach the maximum. This phenomenon also verifies a fact that the energy of dark is strong. Then the rogue wave will disappear and there will left the dark soliton and the breather.

### 5. Summary and Conclusions

In this paper, by using the KP hierarchy method, we construct some localized waves and the interactions between them. We start with two different kinds of breather and derive some interesting solutions. Since these two kinds of breathers have different periodicities and localities, they will reduce to some very different types of solutions. For example, the first breather will reduce to the homoclinic orbits solution and the second type of breather will reduce the solitons. For these solutions, we give some figures to exhibit the dynamics of these dynamics. And we find some very interesting interactions about them. The interaction between the dark soliton and the anti-dark soliton looks like a resonance soliton at a fixed time.

Moreover, by using the long wave limit skill, we can derive the lump solution and the rogue wave from these two kinds of breathers. Due to the difference of breathers, the corresponding semi-rational solutions will also be quite different. In the Appendixes, we present all kinds of solutions. By choosing different orders, we can get different solutions.

Especially, we give an amazing phenomenon composed by the rogue wave, breather and dark soliton and we give a detailed analysis for it.

In our paper, we only give the multi-solitons with the KP reduction method. Another high-order solutions are also important in the integrable system. But it is difficult to construct the interaction between the high-order rogue waves and breather solutions since these two kinds of waves are obtained under two different reduction conditions. In addition, there are some integrable fractional equation, we can try to study these topics in the next work.

**Author Contributions:** Conceptualization, H.-H.D. and Y.Z.; methodology, H.-H.D. and Y.F.; software, Y.Z.; validation, H.-H.D. and Y.F.; formal analysis, Y.Z.; investigation, Y.Z.; writing—original draft preparation, Y.F.; project administration, H.-H.D. All authors have read and agreed to the published version of the manuscript.

**Funding:** This work was supported by the Natural Science Foundation of Shandong Province (Grant No. ZR2019QD018), National Natural Science Foundation of China (Grant No. 11975143, 12105161, 61602188), CAS Key Laboratory of Science and Technology on Operational Oceanography (Grant No. OOST2021-05), Scientific Research Foundation of Shandong University of Science and Technology for Recruited Talents (Grant No. 2017RCJJ068, 2017RCJJ069).

**Institutional Review Board Statement:** Not applicable.

**Informed Consent Statement:** Not applicable.

**Data Availability Statement:** Not applicable.

**Acknowledgments:** We would like to express their thanks to the editors and the reviewers for their kind comments to improve our paper.

**Conflicts of Interest:** The authors declare no conflict of interest.

## Appendix A

With the theory in Ref. [24], we know that the parameters  $\mu_i, \omega_j$  have two different choices, one is

$$\mu_{2k-1} = -\Phi_k + \frac{\phi_k}{2}, \mu_{2k} = -\Phi_k^* - \frac{\phi_k}{2}, \omega_{2k-1} = \Phi_k + \frac{\phi_k}{2}, \omega_{2k} = \Phi_k^* - \frac{\phi_k}{2} \quad (\text{A1})$$

and  $\zeta_{2k-1,0} = \zeta_{2k,0} \equiv \zeta_{k,0}, \eta_{2k-1,0} = \eta_{2k,0} \equiv \eta_{k,0}, \Phi_k$  are complex parameters,  $\phi_k, \xi_{k,0}, \eta_{k,0}$  are all real parameters. Then the breathers to the Maccari system can be given as

$$A = \frac{g \exp(-ibt)g}{f}, \quad (\text{A2})$$

$$u = 2(\ln f)_{xx} - b$$

where  $f = \Delta |F_{k,l}|, g = \Delta |G_{k,l}|$ , and  $\Delta = \exp(\sum_{i=1}^M \Psi_i + \Psi_i^*) \prod_{k=1}^M \phi_k^2, F_{k,l}, G_{k,l}$  are defined as

$$\begin{aligned}
 F_{k,k} &= \begin{bmatrix} \frac{1}{\phi_k \exp(\Psi_k)} + \frac{1}{\phi_k} & \frac{-1}{\Phi_k - \Phi_k^*} \\ \frac{-1}{\Phi_k - \Phi_k^*} & \frac{1}{\phi_k \exp(\Psi_k^*)} + \frac{1}{\phi_k} \end{bmatrix} \\
 G_{k,k} &= \begin{bmatrix} \frac{1}{\phi_k \exp(\Psi_k)} + \frac{1}{\phi_k} \frac{\Phi_k + a + \frac{\phi_k}{2}}{\Phi_k + a - \frac{\phi_k}{2}} & \frac{-1}{\Phi_k - \Phi_k^*} \frac{\Phi_k + a - \frac{\phi_k}{2}}{\Phi_k^* + a - \frac{\phi_k}{2}} \\ \frac{-1}{\Phi_k - \Phi_k^*} \frac{\Phi_k^* + a + \frac{\phi_k}{2}}{\Phi_k + a + \frac{\phi_k}{2}} & \frac{1}{\phi_k \exp(\Psi_k^*)} + \frac{1}{\phi_k} \frac{\Phi_k^* + a + \frac{\phi_k}{2}}{\Phi_k^* + a - \frac{\phi_k}{2}} \end{bmatrix} \\
 F_{k,l} &= \begin{bmatrix} \frac{1}{-(\Phi_k - \Phi_l) + \frac{\phi_k + \phi_l}{2}} & \frac{1}{-(\Phi_k - \Phi_l^*) + \frac{\phi_k - \phi_l}{2}} \\ \frac{1}{(\Phi_k^* - \Phi_l) + \frac{\phi_k - \phi_l}{2}} & \frac{1}{(\Phi_k^* - \Phi_l^*) + \frac{\phi_k + \phi_l}{2}} \end{bmatrix} \\
 G_{k,l} &= \begin{bmatrix} \frac{1}{-(\Phi_k - \Phi_l) + \frac{\phi_k + \phi_l}{2}} \frac{\Phi_k + a - \frac{\phi_k}{2}}{\Phi_l + a + \frac{\phi_l}{2}} & \frac{1}{-(\Phi_k - \Phi_l^*) + \frac{\phi_k - \phi_l}{2}} \frac{\Phi_k + a - \frac{\phi_k}{2}}{\Phi_l^* + a - \frac{\phi_l}{2}} \\ \frac{1}{(\Phi_k^* - \Phi_l) + \frac{\phi_k - \phi_l}{2}} \frac{\Phi_k^* + a + \frac{\phi_k}{2}}{\Phi_l + a + \frac{\phi_l}{2}} & \frac{1}{(\Phi_k^* - \Phi_l^*) + \frac{\phi_k + \phi_l}{2}} \frac{\Phi_k^* + a + \frac{\phi_k}{2}}{\Phi_l^* + a - \frac{\phi_l}{2}} \end{bmatrix}
 \end{aligned} \tag{A3}$$

$$\Psi_k = i\phi_k x + 2i\phi_k \Phi_k + t - \frac{2i\phi_k \rho^2}{4\Phi_k^2 - \phi_k^2} y + \Psi_{k,0} \tag{A4}$$

where  $\Phi_k$  are complex parameters, and the parameters  $\phi_k, \zeta_{k,0}, \eta_{k,0}$  are real.

Another choice to the parameters  $\mu_i, \omega_j$  is

$$\mu_{2k-1} = a + \Phi_k, \mu_{2k} = a - \Phi_k, \omega_{2k-1} = -a + \Phi_k^*, \omega_{2k} = -a - \Phi_k^*,$$

which also satisfies the constraint condition  $\tilde{g} = g^*$  under  $N$  in Equation (5) in even. For these two choices of parameters, we know that the second breather is connected with the first one under some parameterization constraints. Then we only give a analysis for the first case, the other one can be given similarly.

### Appendix B

To derive the rational solution, we should use some limiting skill. From the exact solution in Equation (A2), if we set the hypothesis  $\exp(\Psi_{i,0}) = -1$  and calculate under the limit  $\phi_i \rightarrow 0$ , we can get the rational solutions. The details are as follows:

The rational solution to Maccari system Equation (3) is

$$\begin{aligned}
 A &= \frac{\rho \exp(-ibt)g}{f}, \\
 u &= 2(\ln f)_{xx} - b,
 \end{aligned} \tag{A5}$$

where  $f = |F_{k,l}|, g = |G_{k,l}|$  and the entries is defined as

$$\begin{aligned}
 F_{k,k} &= \begin{bmatrix} \omega_k & \frac{-1}{\Phi_k - \Phi_k^*} \\ \frac{-1}{\Phi_k - \Phi_k^*} & \omega_k^* \end{bmatrix} \\
 G_{k,k} &= \begin{bmatrix} \omega_k - \frac{1}{\Phi_k + a} & \frac{-1}{\Phi_k - \Phi_k^*} \frac{\Phi_k + a}{\Phi_k^* + a} \\ \frac{-1}{\Phi_k - \Phi_k^*} \frac{\Phi_k^* + a}{\Phi_k + a} & \omega_k^* + \frac{1}{\Phi_k^* + a} \end{bmatrix} \\
 F_{k,l} &= \begin{bmatrix} \frac{1}{-(\Phi_k - \Phi_l)} & \frac{1}{-(\Phi_k - \Phi_l^*)} \\ \frac{1}{\Phi_k^* - \Phi_l} & \frac{1}{\Phi_k^* - \Phi_l^*} \end{bmatrix} \\
 G_{k,l} &= \begin{bmatrix} \frac{1}{-(\Phi_k - \Phi_l)} \frac{\Phi_k + a}{\Phi_l + a} & \frac{1}{-(\Phi_k - \Phi_l^*)} \frac{\Phi_k + a}{\Phi_l^* + a} \\ \frac{1}{\Phi_k^* - \Phi_l} \frac{\Phi_k^* + a}{\Phi_l + a} & \frac{1}{\Phi_k^* - \Phi_l^*} \frac{\Phi_k^* + a}{\Phi_l^* + a} \end{bmatrix}
 \end{aligned} \tag{A6}$$

where

$$\omega_k = ix + 2i\Phi_k + t - \frac{2i\varrho^2}{4\Phi_k^2}y.$$

### Appendix C

Now that there are rational solution and exp-type solution, it must exist the semi-rational solution, i.e., the mixed rational-exp solution to Maccari system.

Moreover, we can give the mixed solutions of the rational solution and the exponential solution. Without loss of generality, we give  $\hat{N}$ -rational solution and  $\tilde{N}$ -exp solution by combining the solution in Equations (A3) and (A6),

$$\begin{aligned} A &= \frac{\varrho \exp(-ibt)g}{f}, \\ u &= 2(\ln f)_{xx} - b, \end{aligned} \tag{A7}$$

where  $f = \Delta_0|F_{k,l}|, g = \Delta_0|G_{k,l}|$  and  $\Delta_0 = \exp(\sum_{k=1}^{\tilde{N}} \Psi_k + \Psi_k^*) \prod_{k=1}^{\tilde{N}} \phi_k^2$ , the entries of these matrices are defined as

$$|F_{k,l}| = \begin{vmatrix} \hat{F} & \check{F} \\ \check{F} & \hat{F} \end{vmatrix}, \quad |G_{k,l}| = \begin{vmatrix} \hat{G} & \check{G} \\ \check{G} & \hat{G} \end{vmatrix}, \tag{A8}$$

where the matrix elements are

$$\begin{aligned}
 \hat{F}_{k,k} &= \begin{bmatrix} \omega_k & \frac{-1}{\Phi_k - \Phi_k^*} \\ \frac{-1}{\Phi_k - \Phi_k^*} & \omega_k^* \end{bmatrix}, \\
 \hat{G}_{k,k} &= \begin{bmatrix} \omega_k - \frac{1}{\Phi_k + a} & \frac{-1}{\Phi_k - \Phi_k^*} \frac{\Phi_k + a}{\Phi_k^* + a} \\ \frac{-1}{\Phi_k - \Phi_k^*} \frac{\Phi_k^* + a}{\Phi_k + a} & \omega_k^* + \frac{1}{\Phi_k^* + a} \end{bmatrix}, \\
 \hat{F}_{k,l} &= \begin{bmatrix} \frac{1}{-(\Phi_k - \Phi_l)} & \frac{1}{-(\Phi_k - \Phi_l^*)} \\ \frac{1}{\Phi_k^* - \Phi_l} & \frac{1}{\Phi_k^* - \Phi_l^*} \end{bmatrix}, \\
 \hat{G}_{k,l} &= \begin{bmatrix} \frac{1}{-(\Phi_k - \Phi_l)} \frac{\Phi_k + a}{\Phi_l + a} & \frac{1}{-(\Phi_k - \Phi_l^*)} \frac{\Phi_k + a}{\Phi_l^* + a} \\ \frac{1}{\Phi_k^* - \Phi_l} \frac{\Phi_k^* + a}{\Phi_l + a} & \frac{1}{\Phi_k^* - \Phi_l^*} \frac{\Phi_k^* + a}{\Phi_l^* + a} \end{bmatrix}, \\
 \check{F}_{k,l} &= \begin{bmatrix} \frac{1}{-(\Phi_k - \Phi_l) + \frac{\phi_l}{2}} & \frac{1}{-(\Phi_k - \Phi_l^*) - \frac{\phi_l}{2}} \\ \frac{1}{(\Phi_k^* - \Phi_l) - \frac{\phi_l}{2}} & \frac{1}{(\Phi_k^* - \Phi_l^*) + \frac{\phi_l}{2}} \end{bmatrix}, \\
 \check{G}_{k,l} &= \begin{bmatrix} \frac{1}{-(\Phi_k - \Phi_l) + \frac{\phi_l}{2}} \frac{\Phi_k + a}{\Phi_l + a + \frac{\phi_l}{2}} & \frac{1}{-(\Phi_k - \Phi_l^*) - \frac{\phi_l}{2}} \frac{\Phi_k + a}{\Phi_l^* + a - \frac{\phi_l}{2}} \\ \frac{1}{(\Phi_k^* - \Phi_l) - \frac{\phi_l}{2}} \frac{\Phi_k^* + a}{\Phi_l + a + \frac{\phi_l}{2}} & \frac{1}{(\Phi_k^* - \Phi_l^*) + \frac{\phi_l}{2}} \frac{\Phi_k^* + a}{\Phi_l^* + a - \frac{\phi_l}{2}} \end{bmatrix}, \\
 \check{F}_{k,l} &= \begin{bmatrix} \frac{1}{-(\Phi_k - \Phi_l) + \frac{\phi_k}{2}} & \frac{1}{-(\Phi_k - \Phi_l^*) + \frac{\phi_k}{2}} \\ \frac{1}{(\Phi_k^* - \Phi_l) + \frac{\phi_k}{2}} & \frac{1}{(\Phi_k^* - \Phi_l^*) + \frac{\phi_k}{2}} \end{bmatrix}, \\
 \check{G}_{k,l} &= \begin{bmatrix} \frac{1}{-(\Phi_k - \Phi_l) + \frac{\phi_k}{2}} \frac{\Phi_k + a - \frac{\phi_k}{2}}{\Phi_l + a} & \frac{1}{-(\Phi_k - \Phi_l^*) + \frac{\phi_k}{2}} \frac{\Phi_k + a - \frac{\phi_k}{2}}{\Phi_l^* + a} \\ \frac{1}{(\Phi_k^* - \Phi_l) + \frac{\phi_k}{2}} \frac{\Phi_k^* + a + \frac{\phi_k}{2}}{\Phi_l + a} & \frac{1}{(\Phi_k^* - \Phi_l^*) + \frac{\phi_k}{2}} \frac{\Phi_k^* + a + \frac{\phi_k}{2}}{\Phi_l^* + a} \end{bmatrix}, \\
 \acute{F}_{k,k} &= \begin{bmatrix} \frac{1}{\phi_k \exp(\Psi_k)} + \frac{1}{\phi_k} & \frac{-1}{\Phi_k - \Phi_k^*} \\ \frac{-1}{\Phi_k - \Phi_k^*} & \frac{1}{\phi_k \exp(\Psi_k^*)} + \frac{1}{\phi_k} \end{bmatrix}, \\
 \acute{G}_{k,k} &= \begin{bmatrix} \frac{1}{\phi_k \exp(\Psi_k)} + \frac{1}{\phi_k} \frac{\Phi_k + a - \frac{\phi_k}{2}}{\Phi_k + a + \frac{\phi_k}{2}} & \frac{-1}{\Phi_k - \Phi_k^*} \frac{\Phi_k + a - \frac{\phi_k}{2}}{\Phi_k + a - \frac{\phi_k}{2}} \\ \frac{-1}{\Phi_k - \Phi_k^*} \frac{\Phi_k + a + \frac{\phi_k}{2}}{\Phi_k + a + \frac{\phi_k}{2}} & \frac{1}{\phi_k \exp(\Psi_k^*)} + \frac{1}{\phi_k} \frac{\Phi_k + a + \frac{\phi_k}{2}}{\Phi_k + a - \frac{\phi_k}{2}} \end{bmatrix}, \\
 \acute{F}_{k,l} &= \begin{bmatrix} \frac{1}{-(\Phi_k - \Phi_l) + \frac{\phi_k + \phi_l}{2}} & \frac{1}{-(\Phi_k - \Phi_l^*) + \frac{\phi_k - \phi_l}{2}} \\ \frac{1}{(\Phi_k^* - \Phi_l) + \frac{\phi_k - \phi_l}{2}} & \frac{1}{(\Phi_k^* - \Phi_l^*) + \frac{\phi_k + \phi_l}{2}} \end{bmatrix}, \\
 \acute{G}_{k,l} &= \begin{bmatrix} \frac{1}{-(\Phi_k - \Phi_l) + \frac{\phi_k + \phi_l}{2}} \frac{\Phi_k + a - \frac{\phi_k}{2}}{\Phi_l + a + \frac{\phi_l}{2}} & \frac{1}{-(\Phi_k - \Phi_l^*) + \frac{\phi_k - \phi_l}{2}} \frac{\Phi_k + a - \frac{\phi_k}{2}}{\Phi_l^* + a - \frac{\phi_l}{2}} \\ \frac{1}{(\Phi_k^* - \Phi_l) + \frac{\phi_k - \phi_l}{2}} \frac{\Phi_k + a + \frac{\phi_k}{2}}{\Phi_l + a + \frac{\phi_l}{2}} & \frac{1}{(\Phi_k^* - \Phi_l^*) + \frac{\phi_k + \phi_l}{2}} \frac{\Phi_k^* + a + \frac{\phi_k}{2}}{\Phi_l^* + a - \frac{\phi_l}{2}} \end{bmatrix},
 \end{aligned}
 \tag{A9}$$

where

$$\begin{aligned}
 \omega_k &= ix + 2i\Phi_k t - \frac{2i\varrho^2}{4\Phi_k^2} y, \\
 \Psi_k &= i\phi_k x + 2i\phi_k \Phi_k t - \frac{2i\phi_k \varrho^2}{4\Phi_k^2 - \phi_k^2} y + \Psi_{k,0}
 \end{aligned}
 \tag{A10}$$

### Appendix D

In this case, we choose the parameters as

$$\mu_{2k-1} = i\left(-\Phi_k + \frac{\phi_k}{2}\right), \mu_{2k} = -i\left(\Phi_k^* + \frac{\phi_k}{2}\right), \omega_{2k-1} = i\left(\Phi_k + \frac{\phi_k}{2}\right), \omega_{2k} = -i\left(\Phi_k^* - \frac{\phi_k}{2}\right) \tag{A11}$$

and  $\zeta_{2k-1,0} = \zeta_{2k,0} = \zeta_{k,0}, \eta_{2k-1,0} = \eta_{2k,0} = \eta_{k,0}$ .  $\Phi_k$  in this case are still complex and  $\phi_k, \zeta_{k,0}, \eta_{k,0}$  are real. Then

$$\begin{aligned} \zeta_{2k-1} + \eta_{2k-1} &= \zeta_{2k}^* + \eta_{2k}^* \\ &= -\phi_{2k}x - 2i\phi_{2k}\Phi_{2k}t - \frac{2\phi_{2k}\varrho^2}{\phi_{2k}^2 - 4\Phi_{2k}^2}y + \zeta_{k,0} + \eta_{1,0}. \end{aligned}$$

Under this choice, we can get another breathers for the Maccari system,

$$\begin{aligned} A &= \frac{\varrho \exp(-ibt)g}{f}, \\ u &= 2(\ln(\exp(\Psi_2 + \Psi_2^*)\phi_2^2) \cdot f)_{xx} - b, \end{aligned} \tag{A12}$$

where  $f = \Delta|F_{k,l}|, g = \Delta|G_{k,l}|$ , and  $\Delta = \exp(\sum_{i=1}^M \Psi_i + \Psi_i^*) \prod_{k=1}^M \phi_k^2$ ,  $F_{k,l}, G_{k,l}$  are defined as

$$\begin{aligned} F_{k,k} &= \begin{bmatrix} \frac{-i}{\phi_k \exp(\Psi_k)} + \frac{-i}{\phi_k} & \frac{i}{\Phi_k + \Phi_k^* - \phi_k} \\ \frac{i}{\Phi_k + \Phi_k^* + \phi_k} & \frac{i}{\phi_k \exp(\Psi_k^*)} + \frac{i}{\phi_k} \end{bmatrix} \\ G_{k,k} &= \begin{bmatrix} \frac{-i}{\phi_k \exp(\Psi_k)} + \frac{-i}{\phi_k} \frac{\Phi_k - ia - \frac{\phi_k}{2}}{\Phi_k - ia + \frac{\phi_k}{2}} & \frac{i}{\Phi_k + \Phi_k^* - \phi_k} \frac{\Phi_k - ia - \frac{\phi_k}{2}}{-\Phi_k^* - ia + \frac{\phi_k}{2}} \\ \frac{i}{\Phi_k + \Phi_k^* + \phi_k} \frac{\Phi_k^* + ia + \frac{\phi_k}{2}}{-\Phi_k + ia - \frac{\phi_k}{2}} & \frac{i}{\phi_k \exp(\Psi_k^*)} + \frac{i}{\phi_k} \frac{\Phi_k^* + ia + \frac{\phi_k}{2}}{\Phi_k^* + ia - \frac{\phi_k}{2}} \end{bmatrix} \\ F_{k,l} &= \begin{bmatrix} \frac{i}{\Phi_k - \Phi_l - \frac{\phi_k + \phi_l}{2}} & \frac{i}{\Phi_k + \Phi_l^* - \frac{\phi_k + \phi_l}{2}} \\ \frac{i}{(\Phi_k^* + \Phi_l) + \frac{\phi_k + \phi_l}{2}} & \frac{i}{(\Phi_k^* - \Phi_l^*) + \frac{\phi_k + \phi_l}{2}} \end{bmatrix} \\ G_{k,l} &= \begin{bmatrix} \frac{i}{\Phi_k - \Phi_l + \frac{\phi_k - \phi_l}{2}} \frac{\Phi_k - ia - \frac{\phi_k}{2}}{\Phi_l - ia + \frac{\phi_l}{2}} & \frac{i}{\Phi_k + \Phi_l^* - \frac{\phi_k + \phi_l}{2}} \frac{\Phi_k - ia - \frac{\phi_k}{2}}{-\Phi_l^* - ia + \frac{\phi_l}{2}} \\ \frac{i}{(\Phi_k^* + \Phi_l) + \frac{\phi_k + \phi_l}{2}} \frac{\Phi_k^* + ia + \frac{\phi_k}{2}}{-\Phi_l + ia - \frac{\phi_l}{2}} & \frac{i}{(\Phi_k^* - \Phi_l^*) + \frac{\phi_k + \phi_l}{2}} \frac{\Phi_k^* + ia + \frac{\phi_k}{2}}{\Phi_l^* + ia - \frac{\phi_l}{2}} \end{bmatrix} \end{aligned} \tag{A13}$$

where

$$\Psi_k = -\phi_k x - 2i\phi_k \Phi_k t - \frac{2\phi_k \varrho^2}{\phi_k^2 - 4\Phi_k^2} y + \Psi_{k,0}$$

### Appendix E

For the second type of breather, we can also give the semi-rational solutions with the same method in Appendix C, that is Furthermore, with the same method in Section 3, we give the semi-rational solution as:

$$\begin{aligned} A &= \frac{\varrho \exp(-ibt)g}{f}, \\ u &= 2(\ln f)_{xx} - b, \end{aligned} \tag{A14}$$

where  $f = \Delta_0|F_{k,l}|, g = \Delta_0|G_{k,l}|$  and  $\Delta_0 = \exp(\sum_{k=1}^{\tilde{N}} \Psi_k + \Psi_k^*) \prod_{k=1}^{\tilde{N}} \phi_k^2$  and the entries of matrix is defined as

$$|F_{k,l}| = \begin{vmatrix} \hat{F} & \check{F} \\ \tilde{F} & \acute{F} \end{vmatrix}, \quad |G_{k,l}| = \begin{vmatrix} \hat{G} & \check{G} \\ \tilde{G} & \acute{G} \end{vmatrix} \tag{A15}$$

where the matrix elements are

$$\begin{aligned}
 \hat{F}_{k,k} &= \begin{bmatrix} \omega_k & \frac{i}{\Phi_k + \Phi_k^*} \\ \frac{i}{\Phi_k + \Phi_k^*} & \omega_k^* \end{bmatrix} \\
 \hat{G}_{k,k} &= \begin{bmatrix} \omega_k - \frac{1}{i\Phi_k + a} & \frac{i}{\Phi_k + \Phi_k^*} \frac{-\Phi_k + ia}{\Phi_k^* + ia} \\ \frac{i}{\Phi_k + \Phi_k^*} \frac{-\Phi_k^* - ia}{\Phi_k - ia} & \omega_k^* - \frac{1}{i\Phi_k^* - a} \end{bmatrix} \\
 \hat{F}_{k,l} &= \begin{bmatrix} \frac{i}{\Phi_k - \Phi_l} & \frac{i}{\Phi_k + \Phi_l^*} \\ \frac{i}{\Phi_k^* + \Phi_l} & \frac{i}{\Phi_k^* - \Phi_l^*} \end{bmatrix}, \\
 \hat{G}_{k,l} &= \begin{bmatrix} \frac{i}{\Phi_k - \Phi_l} \frac{i\Phi_k + a}{i\Phi_l + a} & \frac{i}{\Phi_k + \Phi_l^*} \frac{i\Phi_k + a}{-i\Phi_l^* + a} \\ \frac{i}{\Phi_k^* - \Phi_l} \frac{-i\Phi_k^* + a}{i\Phi_l + a} & \frac{i}{\Phi_k^* - \Phi_l^*} \frac{-i\Phi_k^* + a}{-i\Phi_l^* + a} \end{bmatrix}, \\
 \tilde{F}_{k,l} &= \begin{bmatrix} \frac{i}{\Phi_k - \Phi_l - \frac{\phi_l}{2}} & \frac{i}{\Phi_k + \Phi_l^* - \frac{\phi_l}{2}} \\ \frac{i}{(\Phi_k^* + \Phi_l) + \frac{\phi_l}{2}} & \frac{i}{(\Phi_k^* - \Phi_l^*) + \frac{\phi_l}{2}} \end{bmatrix}, \\
 \tilde{G}_{k,l} &= \begin{bmatrix} \frac{i}{\Phi_k - \Phi_l - \frac{\phi_l}{2}} \frac{\Phi_k - ia}{\Phi_l - ia + \frac{\phi_l}{2}} & \frac{i}{\Phi_k + \Phi_l^* - \frac{\phi_l}{2}} \frac{\Phi_k - ia}{-\Phi_l^* - ia + \frac{\phi_l}{2}} \\ \frac{i}{(\Phi_k^* + \Phi_l) + \frac{\phi_l}{2}} \frac{\Phi_k^* + ia}{-\Phi_l + ia - \frac{\phi_l}{2}} & \frac{i}{(\Phi_k^* - \Phi_l^*) + \frac{\phi_l}{2}} \frac{\Phi_k^* + ia}{\Phi_l^* + ia - \frac{\phi_l}{2}} \end{bmatrix}, \\
 \check{F}_{k,l} &= \begin{bmatrix} \frac{i}{\Phi_k - \Phi_l - \frac{\phi_k}{2}} & \frac{i}{\Phi_k + \Phi_l^* - \frac{\phi_k}{2}} \\ \frac{i}{(\Phi_k^* + \Phi_l) + \frac{\phi_k}{2}} & \frac{i}{(\Phi_k^* - \Phi_l^*) + \frac{\phi_k}{2}} \end{bmatrix}, \\
 \check{G}_{k,l} &= \begin{bmatrix} \frac{i}{\Phi_k - \Phi_l - \frac{\phi_k}{2}} \frac{\Phi_k - ia - \frac{\phi_k}{2}}{\Phi_l - ia} & \frac{i}{\Phi_k + \Phi_l^* - \frac{\phi_k}{2}} \frac{\Phi_k - ia - \frac{\phi_k}{2}}{-\Phi_l^* - ia} \\ \frac{i}{(\Phi_k^* + \Phi_l) + \frac{\phi_k}{2}} \frac{\Phi_k^* + ia + \frac{\phi_k}{2}}{-\Phi_l + ia} & \frac{i}{(\Phi_k^* - \Phi_l^*) + \frac{\phi_k}{2}} \frac{\Phi_k^* + ia + \frac{\phi_k}{2}}{\Phi_l^* + ia} \end{bmatrix}, \\
 \acute{F}_{k,k} &= \begin{bmatrix} \frac{-i}{\phi_k \exp(\Psi_k)} + \frac{-i}{\phi_k} & \frac{i}{\Phi_k + \Phi_k^* - \phi_k} \\ \frac{i}{\Phi_k + \Phi_k^* + \phi_k} & \frac{i}{\phi_k \exp(\Psi_k^*)} + \frac{i}{\phi_k} \end{bmatrix}, \\
 \acute{G}_{k,k} &= \begin{bmatrix} \frac{-i}{\phi_k \exp(\Psi_k)} + \frac{-i}{\phi_k} \frac{\Phi_k - ia - \frac{\phi_k}{2}}{\Phi_k - ia + \frac{\phi_k}{2}} & \frac{i}{\Phi_k + \Phi_k^* - \phi_k} \frac{\Phi_k - ia - \frac{\phi_k}{2}}{-\Phi_k^* - ia + \frac{\phi_k}{2}} \\ \frac{i}{\Phi_k + \Phi_k^* + \phi_k} \frac{\Phi_k^* + ia + \frac{\phi_k}{2}}{-\Phi_k + ia - \frac{\phi_k}{2}} & \frac{i}{\phi_k \exp(\Psi_k^*)} + \frac{i}{\phi_k} \frac{\Phi_k^* + ia + \frac{\phi_k}{2}}{\Phi_k^* + ia - \frac{\phi_k}{2}} \end{bmatrix}, \\
 \acute{F}_{k,l} &= \begin{bmatrix} \frac{i}{\Phi_k - \Phi_l - \frac{\phi_k + \phi_l}{2}} & \frac{i}{\Phi_k + \Phi_l^* - \frac{\phi_k + \phi_l}{2}} \\ \frac{i}{(\Phi_k^* + \Phi_l) + \frac{\phi_k + \phi_l}{2}} & \frac{i}{(\Phi_k^* - \Phi_l^*) + \frac{\phi_k + \phi_l}{2}} \end{bmatrix}, \\
 \acute{G}_{k,l} &= \begin{bmatrix} \frac{i}{\Phi_k - \Phi_l + \frac{\phi_k - \phi_l}{2}} \frac{\Phi_k - ia - \frac{\phi_k}{2}}{\Phi_l - ia + \frac{\phi_l}{2}} & \frac{i}{\Phi_k + \Phi_l^* - \frac{\phi_k + \phi_l}{2}} \frac{\Phi_k - ia - \frac{\phi_k}{2}}{-\Phi_l^* - ia + \frac{\phi_l}{2}} \\ \frac{i}{(\Phi_k^* + \Phi_l) + \frac{\phi_k + \phi_l}{2}} \frac{\Phi_k^* + ia + \frac{\phi_k}{2}}{-\Phi_l + ia - \frac{\phi_l}{2}} & \frac{i}{(\Phi_k^* - \Phi_l^*) + \frac{\phi_k + \phi_l}{2}} \frac{\Phi_k^* + ia + \frac{\phi_k}{2}}{\Phi_l^* + ia - \frac{\phi_l}{2}} \end{bmatrix},
 \end{aligned}
 \tag{A16}$$

where

$$\begin{aligned}
 \omega_k &= ix - 2\Phi_k t + \frac{2i\varrho^2}{4\Phi_k^2} y, \\
 \Psi_k &= -\phi_k x - 2i\phi_k \Phi_k t - \frac{2\phi_k \varrho^2}{\phi_k^2 - 4\Phi_k^2} y + \Psi_{k,0}.
 \end{aligned}
 \tag{A17}$$

## References

1. Zabusky, N.J.; Kruskal, M.D. Interaction of soliton in a collisionless plasma and the recurrence of initial states. *Phys. Rev. Lett.* **1965**, *15*, 240–243. [[CrossRef](#)]
2. Yao, R.X.; Li, Y.; Lou, S.Y. A new set and new relations of multiple soliton solutions of (2+1)-dimensional Sawada–Kotera equation. *Commun. Nonlinear Sci.* **2021**, *99*, 105820. [[CrossRef](#)]
3. Wazwaz, A.M.; El-Tantawy, S.A. Solving the (3+1)-dimensional KP-Boussinesq and bKP-boussinesq equations by the simplified Hirota’s method. *Nonlinear Dyn.* **2017**, *88*, 3017–3021. [[CrossRef](#)]
4. Kuznetsov, E.A. Solitons in a parametrically unstable plasma. *Doklady Akademii Nauk SSSR.* **1977**, *22*, 507–508.
5. Palencia, J.L.D. Travelling waves approach in a parabolic coupled system for modelling the behaviour of substances in a fuel tank. *Appl. Sci.* **2021**, *11*, 5846. [[CrossRef](#)]
6. Palencia, J.L.D. Travelling waves and instability in a Fisher–KPP problem with a nonlinear advection and a high-order diffusion. *Eur. Phys. J. Plus* **2021**, *136*, 774. [[CrossRef](#)]
7. Jiao, Y.J.; Yang, J.M.; Zhang, H. Traveling wave solutions to a cubic predator-prey diffusion model with stage structure for the prey. *AIMS Math.* **2022**, *7*, 16261–16277. [[CrossRef](#)]
8. Rahman, S.; Palencia, J.L.D.; González, J.R. Analysis and profiles of travelling wave solutions to a Darcy-Forchheimer fluid formulated with a non-linear diffusion. *AIMS Math.* **2022**, *7*, 15212–15233. [[CrossRef](#)]
9. Palencia, J.L.D.; ur Rahman, S.; Naranjo, A. Analysis of travelling wave solutions for Eyring-Powell fluid formulated with a degenerate diffusivity and a Darcy-Forchheimer law. *AIMS Math.* **2022**, *7*, 6898–6914. [[CrossRef](#)]
10. Zhang, R.F.; Li, M.C.; Albishari, M.; Zheng, F.C.; Lan, Z.Z. Generalized lump solutions, classical lump solutions and rogue waves of the (2+1)-dimensional Caudrey-Dodd-Gibbon-Kotera-Sawada-like equation. *Appl. Math. Comput.* **2021**, *403*, 126201. [[CrossRef](#)]
11. Ma, W.X.; Zhou, Y. Lump solutions to nonlinear partial differential equations via Hirota bilinear forms. *J. Differ. Equations.* **2018**, *264*, 2633–2659. [[CrossRef](#)]
12. Zhang, Y.; Dong, H.H.; Zhang, X.E.; Yang, H.W. Rational solutions and lump solutions to generalized (3+1)-dimensional shallow water-like equation. *Comput. Math. Appl.* **2017**, *73*, 246–252. [[CrossRef](#)]
13. Akhmediev, N.; Ankiewicz, A.; Taki, M. Waves that appear from nowhere and disappear without a trace. *Phys. Lett. A.* **2009**, *373*, 675–678. [[CrossRef](#)]
14. Ankiewicz, A.; Soto-Crespo, J.M.; Akhmediev, N. Rogue waves and rational solutions of the Hirota equation. *Phys. Rev. E.* **2010**, *81*, 046602. [[CrossRef](#)] [[PubMed](#)]
15. Kibler, B.; Fatome, J.; Finot, C.; Millot, G.; Dias, F.; Genty, G.; Akhmediev, N.; Dudley, J.M. The peregrine soliton in nonlinear fibre optics. *Nature Phys.* **2010**, *6*, 790–795. [[CrossRef](#)]
16. Chabchoub, A.; Hoffmann, N.; Onorato, M.; Slunyaev, A.; Sergeeva, A.; Pelinovsky, E.; Akhmediev, N. Observation of hierarchy of up to fifth-order rogue waves in a water Tank. *Phys. Rev. E.* **2012**, *86*, 056601. [[CrossRef](#)]
17. Zhang, X.E.; Chen, Y. Rogue wave and a pair of resonance stripe solitons to a reduced (3+1)-dimensional Jimbo-Miwa equation. *Commun. Nonlinear Sci.* **2017**, *52*, 24–31. [[CrossRef](#)]
18. Zhang, X.E.; Chen, Y. Deformation rogue wave to the (2+1)-dimensional KdV equation. *Nonlinear Dyn.* **2017**, *90*, 755–763. [[CrossRef](#)]
19. Zhang, X.E.; Chen, Y.; Tang, X.Y. Rogue wave and a pair of resonance stripe solitons to a reduced generalized (3+1)-dimensional KP equation. *Comput. Math. Appl.* **2018**, *76*, 1938–1949. [[CrossRef](#)]
20. Yang, B.; Yang, J.K. Rogue waves in (2+1)-dimensional three-wave resonant interactions. *Physica D.* **2022**, *432*, 133160. [[CrossRef](#)]
21. Weng, W.F.; Yan, Z.Y. Inverse scattering and N-triple-pole soliton and breather solutions of the focusing nonlinear Schrödinger hierarchy with nonzero boundary conditions. *Phys. Lett. A* **2021**, *407*, 127472. [[CrossRef](#)]
22. Ma, L.Y.; Zhang, Y.L.; Tang, L.; Shen, S.F. New rational and breather solutions of a higher-order integrable nonlinear Schrödinger equation. *Appl. Math. Lett.* **2021**, *122*, 107539. [[CrossRef](#)]
23. Xu, S.W.; He, J.S. The rogue wave and breather solution of the Gerdjikov-Ivanov equation. *J. Math. Phys.* **2012**, *53*, 063507. [[CrossRef](#)]
24. Chen, J.C.; Feng, B.F.; Maruno, K.I.; Ohta, Y. The derivative Yajima-Oikawa System: Bright, dark soliton and breather solutions. *Stud. Appl. Math.* **2018**, *141*, 145–185. [[CrossRef](#)]
25. Osborne, A.R. Classification of homoclinic rogue wave solutions of the nonlinear Schrödinger equation. *Nat. Hazards Earth Syst. Sci. Discuss.* **2014**, *2*, 897–933.
26. Ablowitz, M.J.; Herbst, B.M. On homoclinic structure and numerically induced chaos for the nonlinear Schrödinger equation. *SIAM J. Appl. Math.* **1990**, *50*, 339–351. [[CrossRef](#)]
27. Maccari, A. Universal and integrable nonlinear evolution systems of equations in 2+1 dimensions. *J. Math. Phys.* **1998**, *38*, 4151–4164. [[CrossRef](#)]
28. Yajima, N.; Oikawa, M. Formation and interaction of sonic-langmuir solitons inverse scattering method. *Prog. Theor. Phys.* **1976**, *56*, 1719–1739. [[CrossRef](#)]
29. Lai, D.W.C.; Chow, K.W. Coalescence of ripplons, breathers, dromions and dark solitons. *J. Phys. Soc. Jan.* **2001**, *70*, 666–677 [[CrossRef](#)]
30. Uthayakumar, A.; Nakkeeran, K.; Porsezian, K. Soliton solution of new (2+1) dimensional nonlinear partial differential equations. *Chaos Soliton. Fract.* **1999**, *10*, 1513–1518. [[CrossRef](#)]

31. Chen, J.C.; Chen, Y.; Feng, B.F.; Maruno, K. General mixed multi-soliton solutions to one-dimensional multicomponent Yajima–Oikawa system. *J. Phys. Soc. Jpn.* **2015**, *84*, 074001. [[CrossRef](#)]
32. Ohta, Y.; Yang, J.K. General high-order rogue waves and their dynamics in the nonlinear Schrödinger equation. *Proc. R. Soc. A* **2012**, *468*, 1716–1740. [[CrossRef](#)]